

IPICYT

**INSTITUTO POTOSINO DE INVESTIGACIÓN
CIENTÍFICA Y TECNOLÓGICA, A.C.**

POSGRADO EN CIENCIAS EN BIOLOGIA MOLECULAR

**Retention of a new-defined intron changes pharmacology
and kinetics of the full-length P2X2 receptor found in
myenteric neurons of the guinea pig**

Tesis que presenta

Andrómeda Liñan Rico

Para obtener el grado de

Doctor en Ciencias en Biología Molecular

Codirectores de la Tesis:

Dr. Carlos Barajas López

Dr. Juan Francisco Jiménez Bremont

San Luis Potosí, S.L.P., 28 de Mayo, 2012



CONSTANCIA DE APROBACIÓN DE LA TESIS

La tesis “*Retention of a new-defined intron changes pharmacology and kinetics of the full-length P2X2 receptor found in myenteric neurons of the guinea pig*” presentada para obtener el grado de Doctor en Biología Molecular fue elaborada por **Andrómeda Liñan Rico** y aprobada el **25 de Abril, 2012** por los suscritos, designados por el Colegio de Profesores de la División de Biología Molecular del Instituto Potosino de Investigación Científica y Tecnológica, A.C.

Dr. Carlos Barajas López
(Codirector de Tesis)

Dr. Juan Francisco Jiménez Bremont
(Codirector de Tesis)

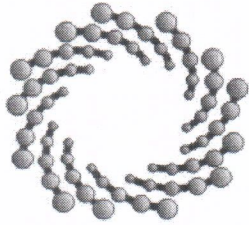
Dr. Jose Jesus García Colunga
(Asesor de Tesis)

Dra. Lina Raquel Riego Ruiz
(Asesor de Tesis)



CREDITOS INSTITUCIONALES

Esta tesis fue elaborada en el Laboratorio de Neurobiología de la División de Biología Molecular del Instituto Potosino de Investigación Científica y Tecnológica A.C. Durante la realización del trabajo el autor recibió una beca académica del Consejo Nacional de Ciencia y Tecnología CONACYT-39129 y del Instituto Potosino de Investigación Científica y Tecnológica, A. C.



IPICYT

Instituto Potosino de Investigación Científica y Tecnológica, A.C.

Acta de Examen de Grado

El Secretario Académico del Instituto Potosino de Investigación Científica y Tecnológica, A.C., certifica que en el Acta 041 del Libro Primero de Actas de Exámenes de Grado del Programa de Doctorado en Ciencias en Biología Molecular está asentado lo siguiente:

En la ciudad de San Luis Potosí a los 28 días del mes de mayo del año 2012, se reunió a las 16:00 horas en las instalaciones del Instituto Potosino de Investigación Científica y Tecnológica, A.C., el Jurado integrado por:

Dr. J. Sergio Casas Flores	Presidente	IPICYT
Dr. Luis Manuel Montaña Ramírez	Secretario	UNAM
Dr. Carlos Barajas López	Sinodal	IPICYT
Dr. José Jesus García Colunga	Sinodal externo	UNAM
Dr. Juan Francisco Jiménez Bremont	Sinodal	IPICYT

a fin de efectuar el examen, que para obtener el Grado de:

DOCTORA EN CIENCIAS EN BIOLOGÍA MOLECULAR

sustentó la C.

Andrómeda Liñan Rico

sobre la Tesis intitulada:

Retention of a new-defined intron changes pharmacology and kinetics of the full-length P2X2 receptor found in myenteric neurons of the guinea pig

que se desarrolló bajo la dirección de

Dr. Carlos Barajas López
Dr. Juan Francisco Jiménez Bremont

El Jurado, después de deliberar, determinó

APROBARLA

Dándose por terminado el acto a las 17:40 horas, procediendo a la firma del Acta los integrantes del Jurado. Dando fe el Secretario Académico del Instituto.

A petición de la interesada y para los fines que a la misma convengan, se extiende el presente documento en la ciudad de San Luis Potosí, S.L.P., México, a los 28 días del mes de mayo de 2012.

Mtra. Ivonne Lizette Cuevas Vélez
Jefa del Departamento del Posgrado

Dr. Marcial Bonilla Marín
Secretario Académico



DEDICACION

A mis padres Marco Agustín Liñan Cabello
y Ofelia Rico Torres

AGRADECIMIENTOS

Al IPICYT por brindarme todos los recursos para mi formación académica.

A CONACYT por la beca otorgada (ALR 39129).

A mis directores de tesis Dr. Carlos Barajas López por haberme dado la oportunidad de trabajar en su laboratorio por su asesoría y el apoyo que me brindó, y al Dr. Juan Francisco Jiménez Bremont por sus enseñanzas y recomendaciones en el área de biología molecular.

A la Dra. Lina Raquel Riego y al Dr. Jesús García Colunga por formar parte de mi comité tutorial y por todas las observaciones y sugerencias que me dieron.

A mis compañeros del laboratorio de neurobiología por sus consejos y amistad. A todos los compañeros de mi generación.

Expreso mi sincero agradecimiento a Rosa Espinosa Luna por todo el apoyo técnico que me brindó a lo largo de mi estancia doctoral, por sus enseñanzas en el manejo de equipo, habilidades técnicas y por todos sus consejos, lo cual fue de mucha ayuda para desarrollar mi proyecto. Agradezco sobretodo por su amistad y porque siempre estuvo dispuesta a apoyarme en todo momento.

Agradezco con mucho cariño a toda mi familia porque siempre me han apoyado, aconsejado y estado al pendiente de mi, agradezco sobretodo a mis padres porque han sido un gran ejemplo para mi y gracias a ellos he logrado mis metas.

CONTENT

CONSTANCIA DE APROBACIÓN DE LA TESIS	II
CREDITOS INSTITUCIONALES	III
ACTA DE EXAMEN.....	IV
DEDICACION	V
AGRADECIMIENTOS.....	VI
LIST OF FIGURES AND TABLES	IX
ABBREVIATIONS.....	X
GLOSSARY	XI
ABSTRACT.....	XII
RETENTION OF A NEW-DEFINED INTRON CHANGES PHARMACOLOGY AND KINETICS OF THE FULL-LENGTH P2X2 RECEPTOR FOUND IN MYENTERIC NEURONS OF THE GUINEA PIG	XII
I. GENERAL BACKGROUND.....	1
1.1 PURINERGIC SIGNALING	1
1.1.2 <i>Type of P2Y receptors</i>	2
1.1.3 <i>Types of P2X receptors</i>	2
1.3 ORGANIZATION OF THE ENTERIC NERVOUS SYSTEM	8
1.4 P2X RECEPTORS IN THE ENTERIC NERVOUS SYSTEM	10
INTRODUCTION	11
P2X2 RECEPTOR IN MYENTERIC NEURONS.....	11
<i>Gene description of P2X2 receptor</i>	13
<i>Pharmacological and biophysical properties of P2X2 receptor</i>	13
THE RATIONALE BEHIND THIS STUDY	20
HYPOTHESIS	21
GENERAL OBJECTIVE	21
MATERIALS AND METHODS	22
GENOMIC SEQUENCE ANALYSIS OF P2X RECEPTORS	22
CLONING OF P2X2 RECEPTOR.....	22
PRIMARY NEURONAL CULTURES	23
SINGLE CELL PCR.....	23
PREPARATION OF XENOPUS LAEVIS OOCYTES	25
ELECTROPHYSIOLOGICAL RECORDINGS.....	26
SOLUTIONS AND REAGENTS	27
DATA ANALYSIS	28
RESULTS	29
ISOLATION AND SEQUENCING OF P2X2 SPLICING VARIANTS OF SMALL INTESTINE.....	29
P2X2-1A AND P2X2-2B VARIANTS	29
<i>Genomic organization of P2x2 gene</i>	31
P2X2-4 NOVEL VARIANT	33
IDENTIFICATION OF P2X2-1, P2X2-2, AND P2X2-4 VARIANTS IN SINGLE MYENTERIC NEURONS BY RT-PCR	36
IONIC CURRENTS MEDIATED BY P2X2 SPLICE VARIANTS EXPRESSED IN OOCYTES	36
EFFECTS OF ANTAGONIST ON P2X2 SPLICE VARIANTS.....	41

DISCUSSION	47
CONCLUSION	52
APPENDIX A	54
APPENDIX B	58
INTRODUCTION	59
MATERIALS AND METHODS	59
<i>Cloning of P2X2 and single cell PCR.....</i>	<i>59</i>
<i>Pharmacological characterization in Xenopus oocytes.....</i>	<i>60</i>
RESULTS	60
APPENDIX C	66
APPENDIX D	68
REFERENCES	69

LIST OF FIGURES AND TABLES

Figure 1. P2X receptor structure.....	5
Figure 2. Homomeric P2X receptors display different desensitization kinetics.....	8
Figure 3. Schematic representation showing the localization of the myenteric plexus at the intestinal wall.....	9
Figure 4. Suramin induced potentiation and inhibition of guinea pig myenteric P2X receptors, but not in mouse.	11
Figure 5. P2X2 receptor is widely distributed at myenteric plexus.....	13
Figure 6. Types of alternative splicing.....	16
Figure 7. General procedure of single cell PCR.	26
Figure 8. Isolation of intestinal P2X2 variants and model of gene structure.....	30
Figure 9. Schematic arrangements of the P2X2 splice variants found in intestine.....	34
Figure 10. Proposed gene model of orthologous <i>P2x2</i> genes.....	35
Figure 11. Genomic organization of P2x paralogous genes..	35
Figure 12. The P2X2 variants are distributed in different proportions in myenteric neurons, being P2X2-1 the most abundant transcript.....	37
Figure 13. P2X2-1 and P2X2-2 form functional homomeric channels with different kinetics.	38
Figure 14. P2X2 splice variants have different sensitivity to ATP and BZATP..	40
Figure 15. α,β -meATP activates both P2X2 receptor variants with very low potency but behaves as an antagonist only at P2X2-1 receptors	42
Figure 16. Suramin inhibits P2X2-1 receptors in a biphasic-manner.....	43
Figure 17. Suramin inhibits P2X2-2 receptors in a monophasic-manner and only at high concentrations.	44
Figure 18. PPADS is clearly more potent on P2X2-1 than on P2X2-2 receptors.....	45
Figure A.1. Desensitization kinetics in <i>Xenopus</i> oocytes coexpressing P2X2-1/P2X2-2GQ suggests the formation of heteromeric channels.....	57
Figure A.2. Coexpressed P2X2-1/P2X2-2GQ subunits showed to types of ATP response.....	57
Figure B.1. Representative agarose gel electrophoresis of P2X2 RT-PCR amplification from intestine (A) or single neurons (B).....	61
Figure B.2. ClustalV alignment of P2X2 cDNA sequences isolated from mouse intestine.....	62
Figure B.3. Murine P2X2-a homomeric receptors respond to ATP in a dependent-concentration manner.....	63
Figure B.4. Murine P2X2-a homomeric receptors display two types of kinetics.....	63
Figure B.5. PPADS and suramin inhibit P2X2-a- receptors with high potency.....	64
Table 1. Summary of the pharmacological properties of homomeric and heteromeric P2X receptors	7
Table 2. Splice variants of P2X2.....	16
Table 3. List of primers used to amplify P2X2 variants	25
Table 4. Properties of homomeric P2X2-1 and P2X2-2 receptors expressed in <i>Xenopus leavis</i> oocytes.....	46

ABBREVIATIONS

aa	Amino acids
α,β-meATP	α,β -methylene ATP
ACh	Acetylcholine
ATP	Adenosine-5'-triphosphate
BzATP	2'-3'-O-(4-benzoylbenzoyl)-ATP
cDNA	Complementary DNA
CNS	Central Nervous System
<i>cpoP2x2</i>	guinea pig <i>P2x2</i> gene
<i>dreP2x2</i>	zebrafish <i>P2x2</i> gene
EC₅₀ (IC₅₀)	Half maximal effective (or inhibitory) concentration
ENS	Enteric Nervous System
fEPSPs	fast excitatory postsynaptic potentials
GABA	γ -aminobutyric acid, 5-hydroxytryptamine
GABA_AR	Receptors GABA _A
GPCRs	G-protein Coupled Receptors
I_{ATP}	ATP-induced currents
nAChR	Nicotinic Acetyl Choline Receptors
NCBI	National Center for Biotechnology Information
NMDG	N-methyl-D- glucamine
ORF	Open Reading Frame
PCR	Polymerase Chain Reaction
PPADS	Pyridoxalphosphate-6-azophenyl-2',4'-disulphonic acid
UTR	Untranslated region
5HT3R	Ionotropic 5-hydroxytryptamine receptor

GLOSSARY

Agonist. Is a chemical that binds and activates a given receptor, triggering a response in the cell.

Antagonist. Is a receptor ligand that does not provoke a biological response by itself but blocks or dampens a cell response induced by an agonist.

Desensitization. Reduction of the cell response induced by an agonist when this is continuously or repetitively administered.

EC₅₀ and IC₅₀. Refers to the concentration of agonist or antagonist that induces a response halfway between the baseline and the maximum after some specified exposure time.

Orthologous gene. Gene in different species that evolved from a common ancestral gene by speciation. Normally, orthologs retain the same function in the course of evolution.

Paralogous genes. Genes related by duplication within a genome. Orthologs retain the same function in the course of evolution, whereas paralogs evolve new functions, even if these are related to the original one.

Stoichiometry. Quantitative relationship of all subunits that conform a given protein, e.g. ion channel.

Hill coefficient. Is a measure of cooperativity during the binding process of the agonists and antagonists to the receptor binding sites. A coefficient of 1 indicates completely independent binding, regardless of how many additional ligands are already bound. Numbers greater than unity indicate positive cooperativity, while less than unity negative cooperativity.

Immunoreactivity. A measure of the immune reaction caused by an antigen.

P2X receptors. Receptor membrane proteins activated by ATP, which include an ion channel.

Two-electrode voltage clamp technique. Is a common electrophysiological technique that allows ion flow across the cell membrane to be measured as an electric current while the transmembrane potential is held constant with a feedback amplifier. Ion channels expressed in *Xenopus* oocytes can be studied using the two-microelectrode voltage clamp technique.

Gq/G11. Heteromeric G protein that activates phospholipase C, thus increasing the levels of the seconds messengers Inositol Trisphosphate and Diacylglycerol.

Gi/o. Heteromeric G protein that inhibits adenylate cyclase activity, decreasing the levels of cAMP.

ABSTRACT

Retention of a new-defined intron changes pharmacology and kinetics of the full-length P2X2 receptor found in myenteric neurons of the guinea pig

P2X2 receptor plays an important role in ATP signaling in guinea pig myenteric plexus. Here, we cloned and characterized three P2X2 isoforms expressed in myenteric neurons. RT-PCR was used to amplify the cDNA of P2X2 variants. These were expressed in *Xenopus* oocytes, and nucleotide-induced membrane currents were recorded with the two-electrode voltage clamp technique.

Three P2X2 cDNAs were identified in myenteric single neurons, named P2X2-1, P2X2-2 and P2X2-4. Based on the analysis of the structural organization of these variants we predicted that P2X2-2 is the fully processed variant, which lead us to propose a new arrangement in the *P2x2* receptor gene with 12 exons and 11 introns. In agreement with this new model, the intron 11 is retained in P2X2-1 and P2X2-4 variants by alternative splicing. Expression of P2X2-1, P2X2-2 and P2X2-4 were found in 92, 42 and 37%, respectively, out of 40 analyzed single neurons. P2X2-4 does not form functional channels, and homomeric channels formed by P2X2-1 and P2X2-2 have a different pharmacological profile. Thus, the former receptor is more sensitive to ATP, BzATP, PPADS, and Zn^{2+} than P2X2-2, whereas, suramin inhibited both receptors but in a biphasic- and monophasic-manner, respectively. α,β -meATP has very low efficacy on either channel. Furthermore, ionic currents mediated by P2X2-1 have slower desensitization than P2X2-2.

P2X2-1 was the most common P2X2 transcript in myenteric neurons and displays significant phenotypical changes implicating that retention of the intron 11 plays a major role in ATP signaling in the intestinal myenteric plexus.

KEYWORDS:

ATP, P2X2 receptors, Alternative splicing, Intron retention, Myenteric neurons, Guinea pig, *P2x2* gene.

RESUMEN

Retención de un nuevo-definido intrón cambia la farmacología y cinética de la isoforma completa del receptor P2X2 encontrado en neuronas mientéricas de cobayo

El receptor P2X2 tiene un papel importante en la señalización purinérgica en el plexo mientérico de cobayo. En este estudio clonamos y caracterizamos tres isoformas del receptor P2X2 que expresan las neuronas mientéricas. Utilizamos la técnica de RT-PCR para amplificar el cDNA de las variantes del P2X2. Las variantes del receptor P2X2 fueron caracterizadas en ovocitos de *Xenopus* y las corrientes de membrana inducidas por nucleótidos fueron registradas con la técnica de pinzamiento del voltaje con dos electrodos.

Identificamos tres cDNAs de la subunidad P2X2 en neuronas mientéricas individuales, nombradas como P2X2-1, P2X2-2 y P2X2-4. Basados en el análisis de la organización estructural de dichas variantes nosotros sugerimos que P2X2-2 es la variante procesada de forma completa, lo cual nos permite proponer un nuevo arreglo del gen del receptor *P2x2* conformado por 12 exones y 11 intrones. De acuerdo a este modelo, las variantes P2X2-1 y P2X2-4 retienen el intrón 11 por splicing alternativo. La expresión de P2X2-1, P2X2-2 y P2X2-4 fue confirmada en el 92, 42 y 37%, respectivamente, de las 40 neuronas individuales analizadas. La subunidad P2X2-4 no forma canales funcionales, mientras que los canales homéricos conformados por las subunidades P2X2-1 y P2X2-2 tienen diferente perfil farmacológico. De ésta forma, el receptor P2X2-1 fue más sensible al ATP, BzATP, PPADS y Zn^{+2} que P2X2-2, mientras que ambos receptores fueron inhibidos por suramin pero de forma bifásica y monofásica, respectivamente. En ambos canales el $\alpha,\beta,\text{meATP}$ mostró muy baja eficacia. Además, las corrientes iónicas mediadas por P2X2-1 mostraron una desensibilización más lenta que los canales P2X2-2.

El transcrito de la subunidad P2X2-1 fue el más común en las neuronas mientéricas y exhibió cambios fenotípicos significativos, lo cual implica que la retención del intron 11 juega un papel importante en la señalización del ATP en el plexo mientérico.

PALABRAS CLAVE

ATP, Receptores P2X2, Splicing alternativo, Retención de intrón, Neuronas mientéricas, Cobayo, Gen *P2x2*.

I. GENERAL BACKGROUND

1.1 Purinergic signaling

The concept of purinergic transmission was initially introduced by Burnstock in 1972 and was received with certain skepticism until the cloning of the first P2 receptor, 20 years (Webb *et al.*, 1993). The proposal of cotransmission, by Burnstock (1976) had also a significant influence on our understanding of neurotransmission, in general, and purinergic cotransmission, in particular. In this sense, there is now a substantial body of evidence showing that ATP is a cotransmitter with ACh, noradrenaline, glutamate, GABA and dopamine in different subpopulations of neurons in the central and peripheral nervous systems (Burnstock, 2009).

The cytoplasm of most cells contains about 2-5 mM ATP. It is now recognized that damaged and healthy cells can release a considerable amount of ATP into the extracellular environment, where it can function as a fast-acting ligand at purinergic receptors. In neurons, one can estimate that peak ATP concentration in the synaptic cleft after the release of a single vesicle may reach ~5–500 μ M (Pankratov *et al.*, 2006). Extracellular ATP is rapidly hydrolyzed by ecto-ATPases and ectonucleotidases and its metabolites (principally adenosine) are also important mediators in cell-signaling. ATP and adenosine act on P2 and P1 receptors, respectively. P1 are G-protein-coupled receptors that are commonly referred to as adenosine receptors (A1R, A2AR, A2BR, γ A3R) (Ralevic *et al.*, 1998). ATP, ADP, UTP and UDP act at P2 receptors, which are either ligand-gated ion channels (P2X) or metabotropic P2Y receptors (Burnstock, 2006).

It is widely recognized that purinergic signaling is a primitive system that is not only involved in neuronal signaling but also in many non-neuronal regulatory processes that include exocrine and endocrine secretion, immune responses, inflammation, pain, platelet aggregation, and endothelial-mediated vasodilatation (Burnstock, 2007; Burnstock *et al.*, 2004). Cell proliferation,

differentiation and death that occur in development and regeneration are also known to be modulated by purinergic receptors (Burnstock, 2002) .

1.1.2 Type of P2Y receptors

P2Y receptors are GPCRs that are activated by low concentrations of ATP (from nM to low μ M range) (North *et al.*, 1997). In mammals, there are at least eight genes encoding subtypes of P2Y receptor. Based on phylogenetic similarity, the presence of amino acids important for ligand binding, and the type of G-protein to which they couple, two distinct P2Y subgroups with a high level of sequence divergence are recognized: the P2Y_{1,2,4,6}, and 11 subgroup and the P2Y_{12,13}, and 14 subgroup (Abbracchio *et al.*, 2006; Burnstock, 2007). Receptors of the first subgroup principally use Gq/G11 that activates the phospholipase C/inositol triphosphate endoplasmic reticulum Ca²⁺-release pathway. The second receptor subgroup, almost exclusively, couple to Gi/o, which inhibits adenylyl cyclase and modulate ion channels (Burnstock, 2007). Thus, ATP binding to P2Y receptors triggers second-messenger cascades that amplify and prolong the duration of the signal over seconds. The characteristics of P2Y and P1 receptors make them appropriate for a long-lasting modulatory function because they can detect lower ATP concentrations over greater distances from the site of release (Khakh, 2001).

1.1.3 Types of P2X receptors

P2X are a family of ligand-gated cationic channels activated by extracellular ATP (in the μ M range). Seven subunits, each codified by a different gene, have been identified so far in mammalian species (P2X₁₋₇) sharing 30-45% identity at the peptide level. In order to assemble a functional channel, P2X subunits form homo or heteromeric trimers (Kawate *et al.*, 2009; Torres *et al.*, 1999).

The P2x gene family. In all *P2rx* orthologous genes of vertebrate species, *P2x4* and *P2x7* subunit genes are localized in closer proximity in the chromosome (in mouse Chr 5) and these are also the closest in amino acid sequence. *P2x1* and *P2x5* are also closely located on the short arm of chromosome 11 (mouse). The remaining genes are all on different chromosomes. The genes vary considerably in size, being *P2x2* the smallest (around 3Kb) and *P2X7* the largest (around 45 Kb) gene. All paralogous genes share a similar structure consisting in 11-13 exons, with well conserved exon-intron boundaries, and also among orthologous *P2x* genes their genomic arrangement is highly conserved. The transcript length of each subunit is around 1.3 Kb (the ORF region). Many spliced forms have been described, mostly for *P2X2* and *P2X7* subunits; the majority of these represent simple forms in which one or more exons are spliced out, or alternative donor/acceptor sites are used (North, 2002).

The evolutionary origin of P2X receptors remains unclear. Despite the high conservation of P2X subunits between vertebrates, the analysis of completely sequenced genomes of non-vertebrate model organisms like *Drosophila melanogaster*, *Caenorhabditis elegans* and *Apis mellifera* showed no homologues to P2X receptors (Burnstock *et al.*, 2009; Fountain *et al.*, 2009). Previous works have hypothesized that ATP was a very early neurotransmitter in evolution of vertebrates (Trams, 1981); however, phylogeny suggests the emergence of seven P2X subunits present in mammals is an early evolutionary event subsequent to the split between vertebrates and invertebrates (Bavan *et al.*, 2009). Nevertheless, there are evidence showing that non-vertebrates like *Schistosoma mansoni* have P2X homologues (Agboh *et al.*, 2004) so it has been proposed that arthropods and nematodes loss their P2X homologues later in their own evolution (Bavan *et al.*, 2009).

Molecular structure of P2X receptors. Members of the family of ionotropic P2X1–7 receptors show a subunit topology of intracellular N- and C-termini of variable lengths (North, 2002). The x-ray crystal have indicated that each subunit consist of two continuous, transmembrane α -helices, intracellular termini and a large disulphide-bond-rich extracellular domain (Kawate *et al.*, 2009). Experimental and structural evidences have showed that the first trasmembrane domain is involved in channel gating and the second is lining the ion pore. The large extracellular loop (~280 aa) contains the ten consensus cysteines that form the disulfide bridges and the consensus amino acids for N-linked glycosylation (Asn-X-Ser/Thr). A hydrophobic region close to the pore vestibule conformed by amino acids of the extracellular loop adjacent to TM1 and TM2, is implicated in channel modulation by protons and ATP-binding (Figure 1A). At the C-terminal, a conserved YXXXX sequence (where “X” is any amino acid) in the juxtamembrane region is involved in membrane retention. Other motifs are involved in endocytosis, permeability changes, binding of lipopolysaccharides, and interactions with other proteins (Khakh *et al.*, 2006; Murrell-Lagnado *et al.*, 2008).

Crystallization of the zP2X4.1R at 3.5-Å resolution showed that the receptor is indeed a trimer (Figure 1B). As described by Kawate et al. (2009), each subunit rises from the plasma membrane, like a dolphin from the surface of the ocean, with its tail submerged within the lipid bilayer. The body regions of three subunits mutually intertwine, forming a central vertical cavity. The ectodomain projects 70 Å above the plasma membrane, and there are three vestibules in the center of the ectodomain. ATP and its analogs likely bind to a non-canonical site ~45Å from the ion channel at the extracellular domain (Kawate *et al.*, 2009).

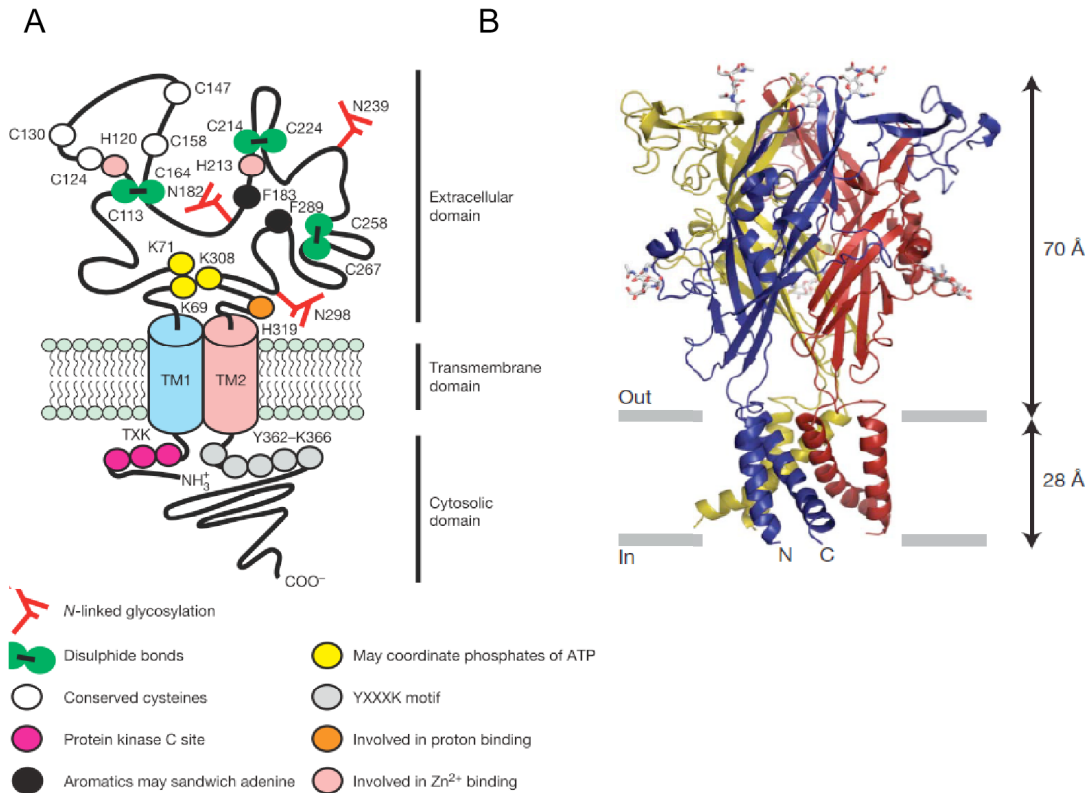


Figure 2. P2X receptor structure. **A)** Topology and key features of P2X receptor subunits, showing the two transmembrane domains, the intracellular N and C terminal region and the extracellular loop. Residues with implications in receptor function and regulation are showed. The numbers are for rat P2X2 receptor (Khakh *et al.*, 2006). **B)** Crystal model of the architecture of P2X receptors. Each subunit is depicted in a different color (Kawate *et al.*, 2009).

Pharmacology of P2X receptors. The pharmacological properties of the assembled P2X receptor vary in function to subunit composition and the species origin of the subunit (Surprenant *et al.*, 1995; Valera *et al.*, 1994). P2X pharmacological characterization has been studied in heterologous expressed channels using *Xenopus* oocytes, HEK293 cells, and insect cells (North *et al.*, 2000). When expressed singly, P2X1 through P2X4 and P2X7 subunits assemble into homomeric channels, which provide robust currents when activated with ATP. With P2X5 receptors the

currents are much smaller. P2X6 do not form functional homomeric channels when expressed in either oocytes or HEK293 cells, primarily due to a failure to even form homo-oligomers. There is both functional and biochemical evidence for P2X receptor formation as heteromultimers, this includes P2X1/P2X4 (Nicke *et al.*, 2005), P2X2/P2X3 (Radford *et al.*, 1997; Torres *et al.*, 1999), P2X1/P2X5, (Le *et al.*, 1999) P2X2/P2X6 (King *et al.*, 2000) and P2X4/P2X6 (Le *et al.*, 1998). P2X7 do not form heteromeric channels (Antonio *et al.*, 2011).

As shown in table 1, homomeric and heteromeric receptors are activated by ATP with EC₅₀ values ranging from 1 to >100 μM. Some agonists (α-β,meATP) and antagonists (TNP-ATP) are selective for some receptors. However, the majority of them are not specific (suramin, PPADS). P2X channels are also modulated by divalent cations (Zn⁺², Ca⁺²), and pH, which might have different modulatory effects on different channels (Roberts *et al.*, 2006).

Table 1. Pharmacological profile of homomeric and heteromeric P2X receptors (Gever *et al.*, 2006).

	P2X1	P2X2	P2X3	P2X4	P2X5	P2X6	P2X7	P2X1/5	P2X2/3	P2X2/6	P2X4/6
Desensitization	Fast	Slow	Fast	Slow	Slow	Slow	Slow	Slow	Slow	Slow	Slow
Agonist EC₅₀ (μM)											
ATP	1	1-30	1	10	10	12	>100	1	1	30	5
ATP-γ-S	3	1-30	0.5	10	10	9	>100	1	1	30	8
α-β-meATP	1	>300	1	>300	>300	>100	>300	1-5	1-3	>100	12
BzATP	0.003	0.75	0.08	7	>500	-	20	-	0.8	-	-
Antagonist IC₅₀ (μM)											
PPADS	1	1	1	>500	≤1	>100	500	≤1	≤4	-	>10
Suramin	1	10	3	>500	≤1	>100	≤50	≤1	≤4	6	≤10
TNP-ATP	0.006	1	0.001	15	-	-	>30	0.4	0.007	-	-

Desensitization of P2X receptors. The decline in the P2X-receptor mediated currents during the continued presence of ATP, or repetitive application of this nucleotide, is named desensitization. In some P2X receptors this decline occurs in milliseconds (fast desensitization: P2X1, P2X3), in others it occurs 100–1,000 times more slowly (slow desensitization: P2X2, P2X4, P2X5), and in P2X7 is absent (Figure 2). Intracellular N and C terminal regions have been shown to influence the rate of receptor desensitization through phosphorylations and interactions with phosphoinositides (Boue-Grabot *et al.*, 2000; Fujiwara *et al.*, 2006; Koshimizu *et al.*, 1999; Nilsen *et al.*, 2010).

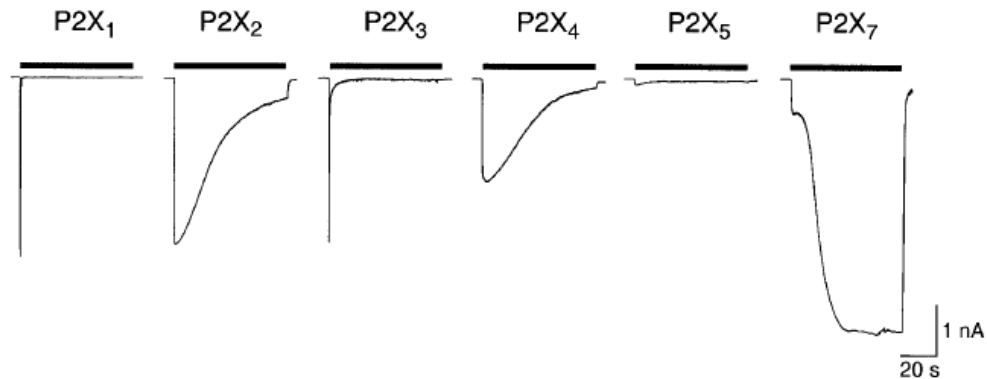


Figure 3. Homomeric P2X receptors display different desensitization kinetics. Prolonged application of ATP (30 μ M, or 1 mM for P2X7) induced currents with fast desensitization only for P2X1 and P2X3 and slow for P2X2 and P2X4. Recordings were done in transfected HEK293 cells with 1 μ g/ml of cDNA (North, 2002).

1.3 Organization of the enteric nervous system

ENS is the division of the autonomic nervous system whose nerve cell bodies and non-neuronal support cells reside entirely within the gut wall. The ENS has as many neurons as the spinal cord and can control gastrointestinal function independent of direct connections with the central nervous system. Enteric nerves perform this function using multiple mechanisms of excitatory and inhibitory neurotransmission in enteric ganglia.

The ENS consists of two ganglionated plexuses: the myenteric and submucosal plexus (Figure 3). The myenteric plexus is between the outer longitudinal and circular muscle layers, and extends the full length of the digestive tract, from the esophagus to the rectum (Furness *et al.*, 1980). The submucosal plexus is prominent only in the small and large intestines. The myenteric plexus controls contractions and relaxations of gastrointestinal smooth muscle (Kunze *et al.*, 1999). The submucosal plexus controls the secretory/absorptive functions of the gastrointestinal

epithelium, local blood flow and neuroimmune responses (Galligan, 2002). Both plexuses contain sensory neurons, interneurons, and motor neurons interconnected by chemical synapses into integrated circuits. Bidirectional communication also occurs between the enteric plexus and the CNS (Brookes, 2001).

There are two broad mechanisms of receptor-mediated excitation and inhibition in the ENS. The first mechanism involves GPCRs. In general, GPCRs mediate slowly developing (onset is longer than 50 ms), but long-lasting (many seconds to minutes), changes in the excitability of enteric neurons. Ligand-gated ion channels are the second broad class of receptor in the ENS; these receptors mediate fast synaptic responses (Khakh, 2001).

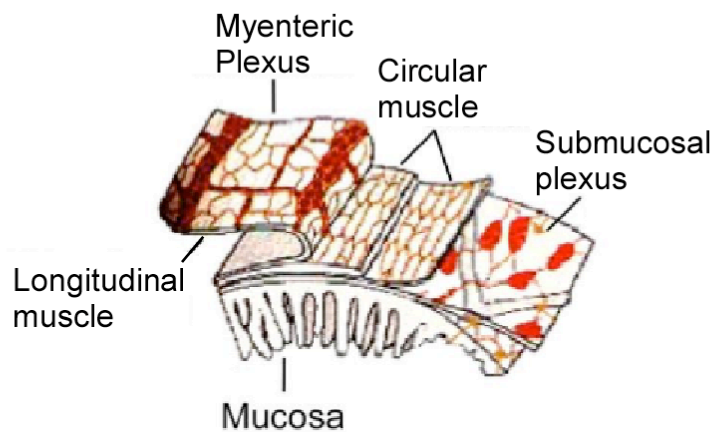


Figure 4. Schematic representation showing the localization of the myenteric plexus in the intestinal wall (modified from Furness et al (1980)).

1.4 P2X receptors in the enteric nervous system

There are two types of neurons in the ENS; S and AH neurons. The S neurons are interneurons and motor neurons, and AH neurons are intrinsic sensory neurons (Brookes, 2001). Exogenously applied adenosine triphosphate (ATP) causes fast fEPSPs in enteric S and AH neurons, indicating that ATP is a fast synaptic transmitter in the myenteric plexus (Barajas-Lopez *et al.*, 1996a; Galligan *et al.*, 1994). Recordings from the duodenum, jejunum, proximal and distal colon revealed that there is a P2X-mediated component to fEPSPs recorded from myenteric neurons in each of these tissues, but that the P2X-mediated component is most prominent in the ileum (Galligan, 2002).

There are controversial findings regarding the pharmacological properties of myenteric P2X receptors, which could reflect the existence of different P2X receptor subtypes and interspecies differences. For instance, suramin, an antagonist for many P2X receptors was reported to potentiate (Barajas-Lopez *et al.*, 1993a; Barajas-Lopez *et al.*, 1996a), inhibit (Galligan *et al.*, 1994) or have no effect (Glushakow *et al.*, 1998) on responses mediated by myenteric P2X receptors of guinea pig small intestine. Our group has shown that in mouse myenteric neurons, I_{ATP} were inhibited by suramin whereas in guinea pig neurons have two effects, potentiation and inhibition of these currents (Figure 4). On guinea pig, both effects of suramin had different recovering kinetics and concentration dependency, indicating that these effects are mediated by at least two different binding sites (Guerrero-Alba *et al.*, 2010).

The presence of at least three P2X subunits in myenteric neurons of the small intestine has been demonstrated. Immunoreactivity for P2X2 (Castelucci *et al.*, 2002), P2X3 (Poole *et al.*, 2002) and P2X7 was reported in guinea pig (Hu *et al.*, 2001). In mouse myenteric neurons, P2X2 (Ren *et al.*, 2003), P2X3 and P2X5 (Ruan *et al.*, 2005) immunoreactivity was detected. However, the

identity of the isoform(s) assembled in these receptors could not be resolved with the antibodies used. The absence of P2X1, P2X4 and P2X6 has been confirmed in guinea pig and mouse (Hu *et al.*, 2001; Ruan *et al.*, 2005).

INTRODUCTION

P2X2 receptor in myenteric neurons

Several lines of evidence strongly suggested that P2X2 is the predominant receptor contributing to the I_{ATP} in myenteric neurons. For instance, in these cells I_{ATP} have kinetics and pharmacological properties that resemble the recombinant rat P2X2 receptor (North, 2002): they have similar desensitization kinetics, show the same sensitivity to ATP and ATP- γ -S, and are highly resistant to α,β -meATP.

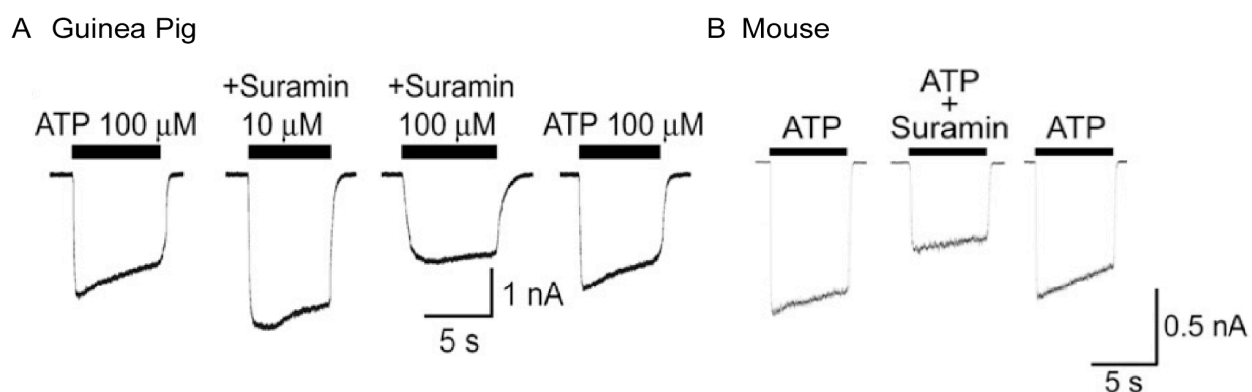


Figure 5. Suramin induced potentiation and inhibition of guinea pig myenteric P2X receptors, but not in mouse. **A)** Inward currents induced by ATP (I_{ATP}) from the same guinea pig cell: before (left trace), during two suramin concentrations and 5 min after suramin removal (right trace). **B)** Recordings of inward currents induced by 1mM ATP, before, in the presence, and 5 min after suramin (30 μ M). Suramin was applied 15 s before ATP. Horizontal bars above traces indicate agonist application (Guerrero-Alba *et al.*, 2010).

Currents with similar properties are found in the great majority of myenteric neurons (>90% of all recorded neurons). In a recent study, we have suggested that in guinea pig myenteric neurons there is a P2X receptor subpopulation that are highly sensitive to ATP (ATP EC₅₀= 38 μM) probably constituted, at least in part, by P2X2 subunits. Additionally, we detected mRNA of P2X2 in a high percentage of myenteric neurons (93%) (Valdez-Morales *et al.*, 2011). At the functional level, Ren *et al.* (2003) showed that homomeric P2X2 channels contribute to fEPSPs in neural pathways underlying peristalsis studied *in vitro* in a mouse knock down model.

P2X2 immunoreactivity was also found at the myenteric plexus. P2X2 receptor expression was detected in specific subtypes of guinea pig myenteric neurons, including inhibitory motor neurons, non-cholinergic secretomotor neurons and intrinsic primary afferent neurons. However, two populations of cells were distinguished having strong and weak immunoreactivity (Figure 5). The proportion of neurons showing weak immunoreactivity was not reported, but 30% of the neurons appear to show strong immunoreactivity (Castelucci *et al.*, 2002). This is in apparent discrepancy with the electrophysiological properties of native myenteric neurons described above, studies that showed robust P2X2-like responses in the majority of cells.

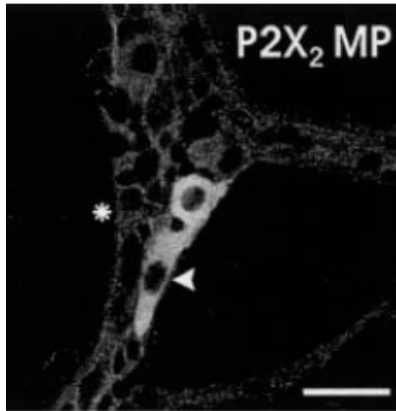


Figure 6. P2X2 receptor is widely distributed at myenteric plexus. Confocal images from myenteric ganglia in the ileum. Neurons with strongly (arrowhead) and weakly immunoreactivity (asterisk) are showed. Bar 25 μm (Castelucci *et al.*, 2002).

Gene description of P2X2 receptor

The mammalian *P2x2* gene is considered to have 11 exons and 10 introns (Brandle *et al.*, 1997), and is located in chr 5 in mouse and chr 12 in rat and human. In Zebrafish a genomic organization consisting of 12 exons and 11 introns was described for *P2x2* gene. In all mammalian species *P2x2* genes is characterized to contain only short introns of 100-300 bp (in others *P2x* genes introns could be as longer as 20 Kb). P2X2 receptor cDNA (P2X2-a) was first isolated from a rat library constructed from NGF-differentiated PC12, and subsequent localization studies have demonstrated a broad tissue distribution. The protein product of this gene consists of 471 amino acids for the fully processed isoform and is well conserved among their orthologous with a protein identity of 75-95%. Several splice variants have been reported in mouse, rat, human and guinea pig (North, 2002).

Pharmacological and biophysical properties of P2X2 receptor

There are no agonists or antagonists that selectively recognize homomeric P2X2 receptors. ATP is a full agonist of P2X2 with a estimate EC_{50} value typically about 10 fold higher than for P2X1

receptors, although there is considerable variability among published values from 2-5 μM (Eickhorst *et al.*, 2002; Li *et al.*, 2004; Zemkova *et al.*, 2004) to 7-60 μM (Brake *et al.*, 1994; Clyne *et al.*, 2003; Evans *et al.*, 1995). They are not activated by α,β -meATP, at least at concentrations up to 300 μM (Table 1), and BzATP behaves as a partial agonist. They are sensitive to suramin and PPADS, but not TNP-ATP. P2X2 is the only one receptor at which the response to ATP is increased by acidification of the extracellular solution. ATP-induced currents are potentiated by both zinc and copper at low micromolar concentrations (North *et al.*, 2000). However different opposite effects have been reported depending the species in the case of modulation by zinc (Tittle *et al.*, 2008).

P2X2 channels exhibit slow desensitization kinetics (Table 1) similar to P2X4 and P2X5. A highly conserved protein kinase C site TX(K/R) located in the intracellular N terminus of P2X subunits has been identified as a critical determinant of kinetics in slowly desensitizing (time constant, >1 min) rat P2X2 receptors (Boue-Grabot *et al.*, 2000). Prolonged or repetitive agonist activation promotes pore dilatation and an increased membrane permeability to larger cations such as NMDG (molecular weight 195 daltons), a characteristic shared by homomeric P2X4 and P2X7 channels (Gever *et al.*, 2006). This increase permeability is known to be due to the movement of subunit cytosolic domains, resulting in a state of high to lower selectivity over the course of 13 s (Eickhorst *et al.*, 2002). For P2X7 channels, this phenomenon has been attributed to the formation of large cytolytic pores in the plasma membrane leading to cell death (Pelegri *et al.*, 2009; Virginio *et al.*, 1999); however, for P2X2 there is no evidence that this mediates cell death.

Alternative splicing of P2X2 receptor

Alternative splicing allows individual genes to produce two or more variant mRNAs, which in many cases encode functionally distinct proteins. Alternative splicing is classified in four major

types (Figure 6): exon skipping; alternative 5' or 3' splice sites; mutually exclusive exons and intron retention (Blencowe, 2006; Fackenthal *et al.*, 2008; Kim *et al.*, 2008). There are others, less frequent, complex events that give rise to alternative transcript variants, including mutually exclusive events, alternative transcription start sites and multiple polyadenylation sites (Kim *et al.*, 2008). P2X2 gene undergoes alternative splicing, some of them with clearly functional implications and others incapable to assemble in a functional homomeric channel (Gever *et al.*, 2006). Table 2 summarizes the P2X2 splice variants that have been reported in mammal species, showing that the P2X2-2 is conserved among all orthologous genes.

In the organ of corti of guinea pig, the fully processed P2X2 subunit and two splice variants have been cloned: P2X2-1, P2X2-2 and P2X2-3 (Parker *et al.*, 1998). Subunits P2X2-1 and P2X2-2 differ in the length of the C-terminal domain, being P2X2-1 64 amino acids longer. P2X2-3 variant has an additional 27 amino acids at the extracellular loop due to a retained intron. The three isoforms are capable to form homomeric receptors with different functional properties. In mouse two splice variants named P2X2-b and P2X2-e were found. P2X2-e variant has even a shorter C-terminal region than P2X2-b (Table 2), and, so far, it has not been reported in other species (Koshimizu *et al.*, 2006). In rat, several splice variants have been identified, but only P2X2-2 has been shown to form functional channels that respond to ATP (Brandle *et al.*, 1997). The key difference between homomeric P2X2-1 (or P2X2-1a in mouse) and P2X2-2 (or P2X2-2b in mouse) channels is that the latter has faster desensitization kinetics (ratP2X2b, $\tau = 12-27.5$ s; ratP2X2a, $\tau = 56-115$ s). Human P2X2-2 splice variant with similar amino acid deletion at the C terminus has also been isolated from pituitary tissue, but has identical desensitization characteristics (Lynch *et al.*, 1999). The agonist and antagonist profiles of P2X2 variants have been claimed to be similar, nevertheless, full concentration-response curves have not been done (Chen *et al.*, 2000; Lynch *et al.*, 1999).

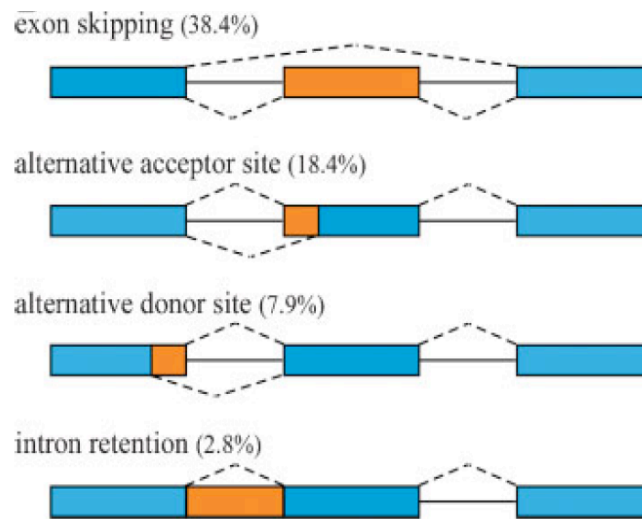


Figure 7. Types of alternative splicing. The four common types of alternative splicing are illustrated. The relative prevalence of each type in alternative exons conserved in human and mouse is shown in parenthesis. The remaining 32.5%, which are not shown, represent more complex alternative splicing events. Constitutive exons are shown in blue; alternatively spliced regions in orange; introns are represented by solid lines; and dashed lines indicate splicing options (Kim et al., 2008).

Table 2. Splice variants of P2X2.

Species	Name	Accession #	Respond to ATP?	Length (aa)	Description
Guinea pig	P2X2-2	AF053328.1	Yes	410	Fragment of 64 aa deleted at exon X
	P2X2-3	AF053329.1	Yes	501	27 aa are inserted due to retention of intron 8
Human	P2X2-b	AAF19171	Yes	404	Fragment of 67 aa missing at exon X
	P2X2-c	AAF19172	No	447	24 aa deleted at exon III
	P2X2-d	AAF19173	No	497	Insertion of 26 aa due to retention of intron 10
	P2X2-h	NP_777361	ND	379	Lacks an in-frame segment of the ORF at exon I, II, III
	P2X2-i	NP_036358	ND	399	Lacks an internal segment of the ORF at exons I, III and IV
Rat	P2X2-2	Y10473	Yes	403	Fragment of 69 aa deleted at exon X
	P2X2-3	AF020756	No	445	27 aa are deleted of exon VI
	P2X2-4*	AF020757	No	166	Retains 46 bp of intron 1 and, exon VI and XI is alternative spliced
	P2X2-5*	AF020758	No	133	Retains 140 bp of intron I, 81 bp deleted at exon XI
	P2X2-6*	AF020759	No	45	19 bp deleted at exon II
	P2X2-c	Y10474	No	466	Deletion of 6 aa at Exon II
	P2X2-d	Y10475	No	484	Retains 36 bp of intron 1
	P2X2-e**	AF028603,	ND	--	92 aa deleted at exon XI
	P2X2-f**	AF028604	ND	--	Fragment of 101 aa deleted at exon XI
	P2X2-g**	AF028605	ND	--	Fragment of 105 aa deleted at exon XI
	P2X2-3R**	AF013241	ND	--	Fragment of 13 aa deleted at exon XI
Mouse	P2X2-b	NP_001158305.1	Yes	416	Segment of 69 aa deleted at exon XI
	P2X2-e	BAC55013	Yes	395	Segment of 90 aa deleted at exon XI

*Splice variant with premature stop codon. **Partial cDNAs. Accession # refers to NCBI protein database. ND, not defined. Guinea pig (Parker *et al.*, 1998), Human (Lynch *et al.*, 1999), Rat (Brake *et al.*, 1994; Brandle *et al.*, 1997; Koshimizu *et al.*, 1998; Salih *et al.*, 1998; Simon *et al.*, 1997; Troyanovskaya *et al.*, 1998), Mouse (Koshimizu *et al.*, 2006).

Protein interactions of P2X2 receptor

The large C-terminal region of P2X2-1 subunit contain regulatory motif involved in proteins interactions. Yeast 2-hybrid analysis has shown that the scaffolding protein Fe65 interacts with P2X2 receptor, and proline rich regions at the C-terminal are the probably binding site (Guimaraes, 2008; Masin *et al.*, 2006). The assembly with Fe65 regulates the functional properties of P2X2 receptors. Thus, the time and activation dependent change in ionic selectivity (pore dilatation) of P2X2 receptor was inhibited when is coexpressed with Fe65, suggesting a novel role for Fe65 in regulating P2X receptor function and ATP-mediated synaptic transmission. No interaction was observed between Fe65 and the splice variant P2X2-2, indicating that alternative splicing regulates the receptor complex assembly (Masin *et al.*, 2006). However, a specific interaction between the P2X2-1 isoform and β -tubulin I was demonstrated, being the amino acids 378-379 the region responsible for this, which shows a functional interaction between P2X2-1 and cytoskeleton (Guimaraes, 2008).

P2X2 binding to phosphoinositides through the proximal C-terminal cytoplasmic region have been demonstrated to regulate channel desensitization. In the P2X2 C-terminal region a positively charged clustered amino acids are critical for preventing desensitization, and thus maintaining P2X2 channel activity. It was shown that channels enter the desensitized state not from the standard open state, but from the pore-dilated open state, suggesting that the channel phosphoinositide interaction is weakened in the pore-dilated state (Fujiwara *et al.*, 2006).

Functional interactions between P2X2 subunits have also been proposed as a regulatory mechanism. Fujiwara and Kobo (2004) showed that the pore properties of P2X2 channels change dynamically depending on the open channel density. They hypothesized that adjacent open channels are not independent of one other and interactions between them probably through C-

terminal domain, regulated the transition between two different states of the channel (strong and weak rectifier) (Fujiwara *et al.*, 2004). In support to this, interactions between C- and N- termini of P2X2 subunits have been demonstrated with a significant enhanced activity between the shorter forms of P2X2 receptors (mouse P2X2-b and P2X2-e) than with the long isoform (P2X2-a) (Koshimizu *et al.*, 2006).

Another mechanism by which P2X2 channel activity is regulated is the functional interaction with nAChR (Barajas-Lopez *et al.*, 1993b), 5HT3R (Liu *et al.*, 1993) and GABA_AR (Barajas *et al.*, 1993) on the membrane. When P2X2 and these receptors were co-expressed (nAChR 5HT3R or GABA_AR), simultaneous activation of both receptors under voltage clamp evoked membrane current that was clearly smaller than the sum of the currents carried by the two channels individually, indicating direct mutual interaction among the activated channels. These phenomena are reflections of dynamic and flexible features of the P2X2 channel (Barajas-Lopez *et al.*, 1993a).

THE RATIONALE BEHIND THIS STUDY

We have shown that P2X2 receptors are likely the main contributors to the I_{ATP} recorded in myenteric neurons, which is in agreement with recent findings from our laboratory showing the presence of P2X2-mRNA in about 93% of myenteric neurons (Valdez-Morales *et al.*, 2011). In apparent controversy with this, strong P2X2 immunoreactivity has been reported in only 30% of the guinea pig myenteric neurons (Castelucci *et al.*, 2002). A simple explanation for this discrepancy is that myenteric neurons express P2X2 isoform(s) unable to be recognized by the antibody. In an effort to better understand the functional and pharmacological properties of native P2X myenteric channels and their contribution to ATP signaling, in this study we identified and characterized the P2X2 variants expressed by guinea pig myenteric neurons.

HYPOTHESIS

If P2X2-like currents and mRNA for these channels are detected in the great majority (>90%) of myenteric neurons but only 30% of neurons show immunoreactivity, then splice variants of the P2X2 subunit are present in myenteric neurons.

GENERAL OBJECTIVE

Determine the P2X2 variants expressed by guinea pig myenteric neurons and their molecular and functional properties.

SPECIFIC AIMS

1. Clone the P2X2 variants from guinea pig intestine and verified their neuronal origin.
2. Characterize the functional and pharmacological properties of these myenteric P2X2 isoforms.

MATERIALS AND METHODS

Genomic sequence analysis of P2X receptors

Genomic and cDNA sequences encoding P2X2 receptors were obtained from the NCBI (<http://www.ncbi.nlm.nih.gov>) and Ensembl database (<http://www.ensembl.org>). Exon-intron structure of *P2x2* gene was derived from the aligned cDNA/genomic sequence or obtained directly from NCBI.

Cloning of P2X2 receptor

Tissue extracted from thymus and small intestine were triturated in a mortar with liquid nitrogen. The RNAqueous RNA isolation kit (Life Technologies, Texas, USA) was used to obtain total RNA according to the manufacturer's protocol. First strand cDNA were synthesized using Superscript reverse transcriptase II (Life Technologies, Texas, USA) in the presence of oligo (dT)₁₈ for 1.5 h at 42 °C. PCR was performed using specific guinea pig P2X2 primers designed at the 5' and 3' UTRs regions to amplify the entire coding sequence (F1 and R1, see Table 1). PCR reaction was done using Platinum Pfx Taq DNA Polymerase (Life Technologies, Texas, USA), conditions were as follows: initial denaturation for 2 min at 95 °C, then 40 amplification rounds of denaturation for 15 s at 95 °C, alignment for 20 s at 60 °C, and extension for 1 min 45 s at 68 °C; the final extension was 5 min at 68 °C. PCR products were analyzed by electrophoresis in 0.8% agarose gels stained with 1 µg/ml ethidium bromide. Images were obtained with Gel-Doc 2000 Gel Documentation System (Bio-Rad). PCR products were cloned into the pGEM-T Easy Vector (Promega, Wisconsin, USA) sequencing and subcloned in pCDNA3 vector.

Primary neuronal cultures

Guinea pigs (100-150 g) of either sex were sacrificed by cervical dislocation and carotid exsanguination. These methods have been approved by the Animal Care Committee of the IPICYT and are in agreement with the published Guiding Principles in the Care and Use of Animals, approved by the American Physiological Society. Methods for dissection, dissociation and culture of myenteric neurons have been published in detail previously (Barajas-Lopez et al., 1996b). Briefly, a segment of 10-15 cm from the proximal jejunum was removed, placed in modified Krebs solution (in: mM: NaCl, 126; NaH₂PO₄, 1.2; MgCl₂, 1.2; CaCl₂, 2.5; KCl, 5; NaHCO₃, 25; glucose, 11; gassed with 95% O₂ and 5% CO₂) and opened longitudinally. The mucosa and submucosal layers of this intestinal segment were dissected away. In guinea pig, most circular muscle layer can be removed leaving behind the longitudinal layer with the myenteric plexus embedded with it. This myenteric preparation was dissociated using a sequential treatment with two enzymatic solutions. The first solution contained papain (0.01 mg/ml; activated with 0.4 mg/ml L-cysteine) and the second contained collagenase (1 mg/ml) and dispase (4 mg/ml). Enzymes were removed by washing with L15 medium and the neurons were placed on round coverslips coated with sterile rat tail collagen in culture solution, which was composed by minimum essential medium 97.5% (v/v), 2.5% (v/v) guinea pig serum, 15 mM glucose, 2 mM L-glutamine, antibiotics (10 U/ml penicillin, 10 µg/ml streptomycin), and antimetotics (10 µM cytosine-β-D-arabinofuranoside, 10 µM fluorodeoxyuridine and 10 µM uridine) to prevent the growth of non-neuronal cells.

Single cell PCR

We used single myenteric neurons from primary 3-7 days old cultures, which were harvested under visual control into the glass pipette by applying negative pressure. Neurons were differentiated of

other cell types by their round, compact, and bright body from which, long neurites arised (Eclipse TE2000OU, Nikon). This pipette had a tip diameter of about 4-6 μm and contained 6 μl of RNase-free RT buffer (with RNase inhibitor, 20U; oligo (dT)₁₈, 2.3 μM ; dNTPs, 150 μM ; dTT 1.2 mM; 10X RT Buffer Superscript III First-Strand Syntesis System; Life Technologies , Texas, USA). The content of the pipette was expelled into a PCR-tube containing 12 μl of RNase-free RT buffer and 0.5 μl of NP40 1% to allow cell membrane solubilization and the reaction was incubated at 65 $^{\circ}\text{C}$ for 2 min. After adding 0.5 μl reverse transcriptase III, the sample was transferred to 37 $^{\circ}\text{C}$ for 60 min, the reaction was inactivated by heating the sample to 70 $^{\circ}\text{C}$ for 10 min and placed on ice. Negative controls were performed without template; no false amplifications were obtained.

PCR was performed with the same pairs of primers described above using Platinum Taq DNA Polymerase (Life Technologies, Texas, USA) and the PCR protocol were as follows: initial denaturation for 3 min at 94 $^{\circ}\text{C}$, then 30 amplification rounds of denaturation for 15 s at 94 $^{\circ}\text{C}$, alignment for 15 s at 60 $^{\circ}\text{C}$, and extension for 1 min 45 s at 72 $^{\circ}\text{C}$; the final extension was 5 min at 72 $^{\circ}\text{C}$. Two separated reactions of nested PCR with combined primers were done using as a template 1 μl of a 1:10 dilution or 0.3 μl directly of the first PCR. The first reaction distinguished by length P2X2-1 of P2X2-2 using a set of primers 1: the reverse primer R1 and an internal forward primer F2 (see Table 3). The second combination (set 2) discriminated between P2X2-1 and P2X2-4 using the forward primer F1 and an internal reverse primer R2 (Table 3). To increase the specify of the PCR, we performed a third round of amplification combining F2 and R2 (set 3) and changing primers F2 and R2 to F3 and R3 (Table 3), giving a product of 839 (P2X2-1) or 647 bp (P2X2-2) with set 1, 1025 (P2X2-1) or 833 bp (P2X2-4) with set 2 and 1122 bp (P2X2-1) with set 3. A total of 90 cycles of amplification (including the three rounds of amplification) were performed using the same PCR conditions used in the first PCR. The summarized protocol is described in Figure 7. PCR products were confirmed to be P2X2 by sequencing analysis.

Table 3. List of primers used to amplify P2X2 variants

Primer Name	Sequence (5'-3')
F1	GTTCTGGGCACCATGGCTGC
F2	CATCGTGCAGAAGAGCTACCA
F3	TTCACAGAGCTGGCACACAG
R1	TCCTGTCTGCAGACCTGGCGT
R2	GGAGACCAACAACCTTTGCCTG
R3	ATGGTGGGAATCAGGCTGAA

Preparation of Xenopus laevis oocytes

Frogs were anesthetized by immersions in a solution of 10 mM Tricaine (3-aminobenzoic acid ethyl ester) (Sigma-Aldrich, MX) and oocytes were removed by dissection. Oocytes stages V and VI were manually defolliculated and placed in a storage saline solution, containing: extracellular solution (NaCl, 88 mM; KCl, 2 mM; CaCl₂, 1 mM; MgCl₂, 1 mM; and HEPES, 5 mM pH adjusted to 7.2-7.4 with NaOH) supplemented with theophylline (0.5 mM) and piruvic acid (2 mM). Cells were injected with 36 nl of cap and poliA P2X2 mRNA synthesized with T7 mMessage mMachine (Life Technologies, Texas, USA) and incubated at 14 °C for 12-36 h before the electrophysiological experiments.

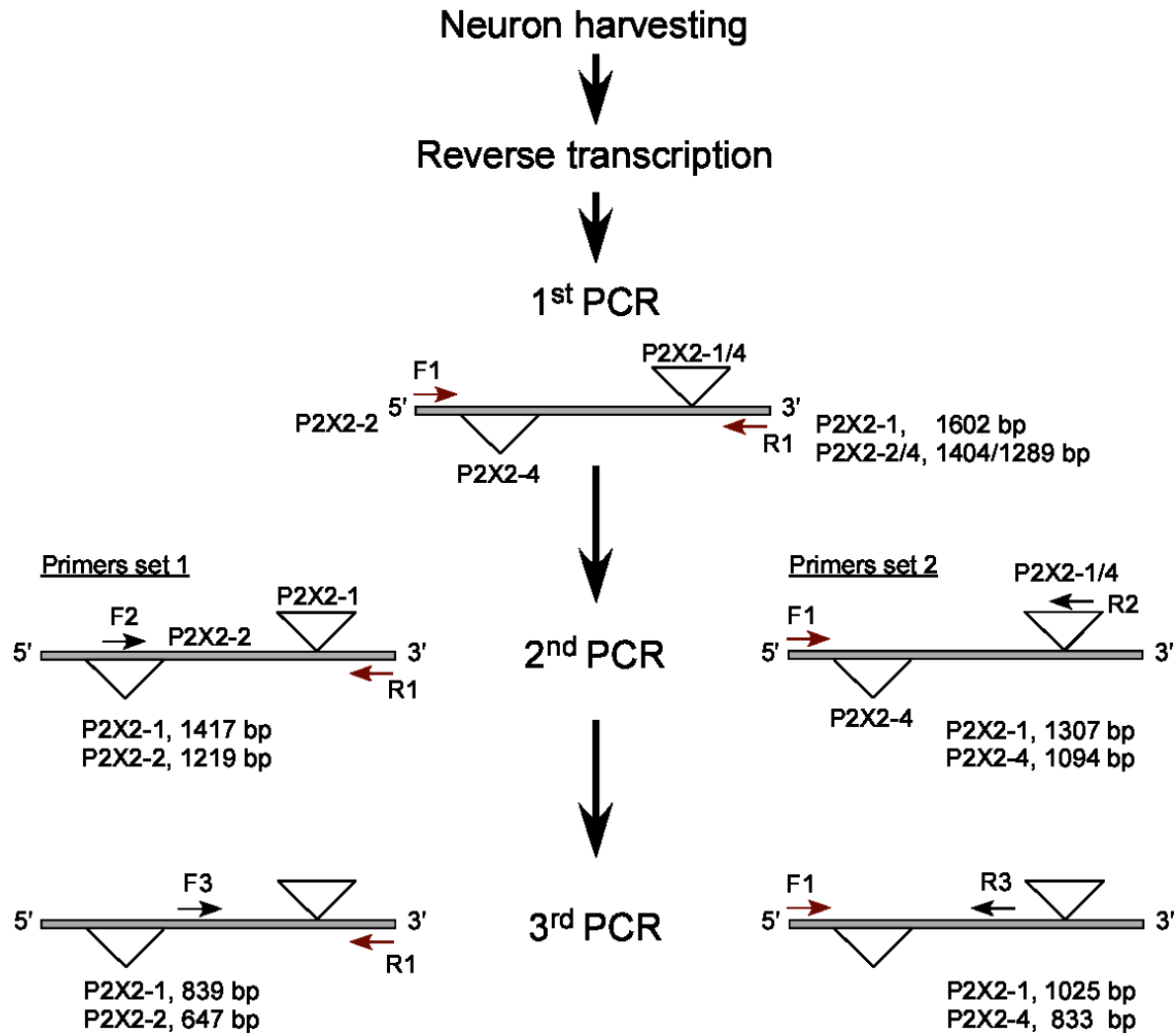


Figure 8. General procedure of single cell PCR. The complete cell is harvested into the pipette, expelled into a test tube and submitted to a reverse transcription step. Next, cDNA are amplified during a first PCR round using primers located at the UTR regions (F1 and R1). Re-amplification through a second round of PCR is performed using two different set of primers: F1-R2 (set 1) and F2-R1 (set 2). Note that primer R2 is located inside intron 11, and therefore P2X2-2 are not amplified. In the same way primer F2 is located at the region that is spliced out in P2X2-4. A third round of amplification increase the definition of the amplification products, in this case primers R2 is changed to R3 and F2 to F3.

Electrophysiological recordings

Membrane currents of oocytes were recorded using the two-electrodes voltage clamp. These electrodes consisted in glass pipettes (0.3-0.8 M Ω resistance) filled with 2 M KCl solution

containing 10 mM EGTA. ATP-induced currents (I_{ATP}) were recorded at a holding potential of -60 mV and at room temperature (22-24 °C). ATP solutions were freshly prepared and maintained in ice to decreased degradation. ATP and its analogs, α,β -meATP and BzATP, were applied usually for 5-15 s or until the current reached its peak. These nucleotides were washout for at least 3 min between consecutive applications. Suramin, PPADS and Zn^{2+} were pre-applied 15 s, 4 min and 2 min, respectively to reach the maximal effect (Guerrero-Alba *et al.*, 2010). Concentration-response curves were constructed using oocytes batches from at least two different frogs. During these electrophysiological experiments the recording chamber was continuously superfused with standard external solution at approximately 3.3 ml/min. The rapid exchange of the external solution around the recorded cell was done using an eight-tube device. Each tube was connected to a syringe containing the control or an experimental solution. The tube containing the control solution was placed in front of the cell being recorded and the external application of substances were applied by abruptly moving another tube in front of the cell, which was already draining the same control solution plus the experimental drug(s). Tubes were moved using a Micromanipulator (WR-88; Narishigie Scientific Instrument Lab, Tokyo Japan).

Substances were removed by returning to the control solution. External solution was released by gravity and the level of the syringes was frequently adjusted to minimize changes in flow rate.

Solutions and reagents

Most salts and substances were all purchased from Sigma-Aldrich (Toluca, MX). ATP stock solution (100 mM) was prepared in extracellular solution freshly every day. The others agonist and antagonists were prepared using deionized water and stored frozen. The desired final drug

concentration was obtained by diluting the stock solutions in extracellular solution before application. The pH was adjusted to 7.4 with NaOH when it was necessary.

L15 medium, Minimum Essential Medium, Hanks solution, penicillin-streptomycin, and L-glutamine were purchased from GIBCO Life Technologies (Texas, USA). Collagenase and papain were bought from Worthington (New Jersey, USA), and dispase from Roche Bioscience (Indianapolis, USA). Theophylline was purchased from Nutritional Biochemistry Corporation (New Jersey, USA). All other salts and substances were all purchased from Sigma-Aldrich (Toluca, MX). Stock solutions (0.01-1 M) were prepared using deionized distilled water and stored frozen. The desired final drug concentration was obtained by diluting the stock solutions in external solution before application.

Data analysis

To normalize the currents induced by ATP, the responses with 300 μ M (for P2X2-1) or 1 mM (for P2X2-2) of this nucleotide were considered as 100%, in each cell. Data are expressed as the mean \pm standard error of the mean (S.E.M.). The number of cells used is represented by "*n*" and concentration-response curves were fitted with a logistic function (Kenakin, 1993).

RESULTS

Isolation and sequencing of P2X2 splicing variants of small intestine

In an attempt to identify the P2X2 variants expressed in the guinea pig small intestine, we designed specific primers for guinea pig P2X2 localized at the 5' and 3' UTR regions in order to amplify the entire ORF. We amplified three P2X2 cDNAs of 1602, 1404, and 1486 bp (Figure 8a), with their corresponding ORF encoding a 477, 411, and 406 amino acids. We submit these cDNA sequences in GenBank as P2X2-1a (FJ641871) P2X2-2b (FJ641872) and P2X2-4 (FJ641873), respectively.

P2X2-1a and P2X2-2b variants

The intestinal splice variant P2X2-1a was 98% identical in nucleotides and 93% in amino acids to the previously reported (P2X2-1, AF053327.1) by Parker (1998), which was isolated from guinea pig organ of corti (Annex 1). The intestinal variant P2X2-2b was almost identical (99% in nucleotides and amino acids) to the one previously registered (P2X2-2, AF053328.1) from organ of corti. Because most of the differences between intestinal variants and those of the organ of corti are located in the C-terminal, we decided to amplify its corresponding genomic fragment contained within the guinea pig *P2x2* gene (*cpoP2x2*) using primers designed to obtain this region (F3 and R1, Table 3). The genomic (the coding sequence) and cDNA sequences that we obtained were identical to genomic sequence subsequently released at Ensembl (ENSCPOG00000013647, Supplementary material). This indicates that the differences between P2X2-1a and P2X2-1 or between P2X2-2b and P2X2-2 sequences are due to errors in the previously described sequences for these two isoforms and therefore, we will refer from now on to the intestinal P2X2-1a and P2X2-2b as P2X2-1 and P2X2-2, respectively.

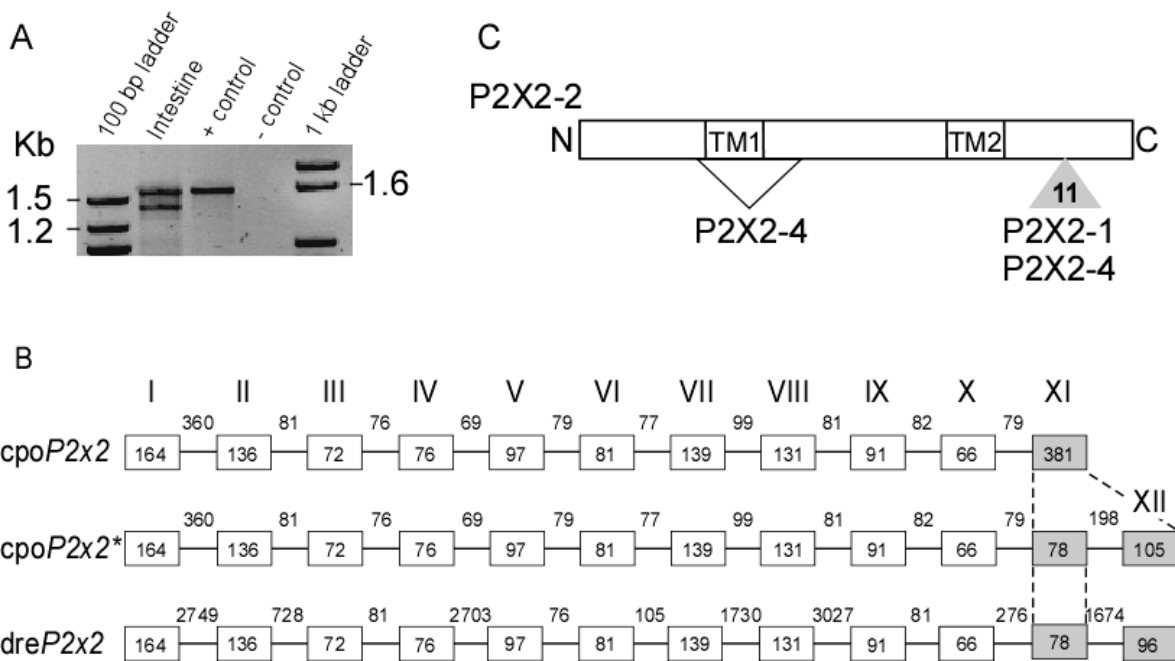


Figure 9. Isolation of intestinal P2X2 variants and model of gene structure. **A)** Agarose gel electrophoresis of P2X2 RT-PCR amplification from intestine. Thymus cDNA was used as positive control and negative control was performed without template. **B)** Schematic representation of *P2x2* gene exon-intron organization. Upper: current organization of guinea pig *P2x2* gene (*cpoP2x2*), consisting of 11 exons and 10 introns. Exons and introns of the ORF region are represented as boxes and lines, respectively. Numbers indicated the length (bp) in each case. Middle: new model of *P2x2* genomic organization (*cpoP2x2**) in which exon XI (marked in gray) are divided in exons XI and XII separated by intron 11. Lower: genomic organization of zebrafish gene (*dreP2x2*), the size of exons and introns are indicated. **C)** Schematic representation of P2X2 protein isoforms structures based in our proposed model of *P2x2* genomic organization. Segment splice out in P2X2-4 is indicated. The gray triangle represents the retained intron in P2X2-4 and P2X2-1 variants. TM1 and TM2 indicate transmembrane regions. Amino (A) and carboxyl (C) terminal regions are represented.

The versions of P2X2 cDNAs previously reported by Parker et al. (1998) have nucleotide changes, and insertions absent in the guinea pig genomic *P2x2* sequence (Ensembl: ENSCPOG00000013647), which modified the amino acid sequence (Annex 1). Relative to P2X2-1 (AF053327.1), these changes were: i) R15A, an insertion of C18 and P37R at the N-terminal; ii) D216E, M217D and T218D at the extracellular loop; iii) finally several nucleotide insertions

changes the ORF in a region of the intracellular C-terminal domain comprising amino acids from 407 to 436.

The only difference in the primary structure of guinea pig P2X2-1 and P2X2-2 variants is the presence of 66 amino acids within the C-terminal region in P2X2-1. These two isoforms are conserved in others mammalian species. However, the P2X2-2 subunit is the only one reported in the zebrafish species (Kucenas *et al.*, 2003). In mammals, this variant had been described to be generated by alternative splicing, where a central segment inside of exon XI is spliced out, generating a shorter version of P2X2 receptor (Brandle *et al.*, 1997). Nevertheless, a splice event where both alternative 5' and 3' splicing are processed within an exon does not correspond to any type of splicing event reported to this date (Blencowe, 2006; Fackenthal *et al.*, 2008; Kim *et al.*, 2008). This observation give us two possibilities, one that the splicing of P2X2-2 was an unusual not described type of splicing event or that P2X2-1 was not the full-length transcript of *P2x2* gene.

Genomic organization of P2x2 gene

Considering the last observations we performed an analysis of the exon-intron organization of the guinea pig *P2x2* gene. The bioinformatic analysis using NetGene2 Server and GENESCAN (Burge *et al.*, 1997; Hebsgaard *et al.*, 1996), predicts intron splice sites flanking the DNA segment that is coding for the 66 amino acids segment present in exon XI of P2X2-1 (data no shown), which prompt us to reorganize the *P2x2* gene structure (exon-intron). We constructed a model of the guinea pig *P2x2* gene structure considering P2X2-2 as the fully processed transcript (Figure 8B). Different to the classical structure proposed for guinea pig *P2x2* gene (*cpoP2x2*) (Figure 8B, upper panel), this new model consists of 12 exons and 11 introns (Figure 8B, middle panel). According with this model, exons XI and XII are divided by a novel 11th intron, which would be constituted

by 198 bp. This last intron is not processed in P2X2-1 variant and therefore, this corresponds to a splicing variant by intron retention. Our new model of *P2x2* gene (*cpoP2x2**) is similar to that proposed for zebrafish *P2x2* gene (*dreP2x2*), which is an orthologous of mammalians P2X2 receptors and also consists of 12 exons and 11 introns (Figure 8B, lower panel).

Altogether these observations indicate that the P2X2-2 transcript corresponds to the complete processed mRNA, and P2X2-1, previously considered as the principal transcript, is a product generated by an event of intron retention (Figure 8C). The retained intron introduces 66 additional amino acids at the C-terminal region of the P2X2-1 variant, as it is indicated in Figures 9A and B.

We next extrapolate the *cpoP2x2* gene model to their mammals' orthologous: mouse, human, rat, monkey and dog. Figure 10 show that the great majority of exons conserve their size, including exon XI (78 bp). Introns are less conserved, intron 11 consist of 197 bp in guinea pig, 201 in human, and 207 bp in the rest of the species. This new arrangement we propose here is more consistent with the current models established for paralogous P2X genes (Figure 11). Taken together, we strongly argue in favor of the P2X2 genomic organization model of 12 exons and 11 introns, implying that P2X2-2 is the full processed transcript.

P2X2-4 novel variant

We found a novel P2X2 splice variant, named P2X2-4, characterized by the presence of three splicing events in the same transcript. The first two splicing types were the use of an alternative 5' splice site in exon I followed by skipping the whole exon II. As seen in the Figure 8C and 9C, the splicing in P2X2-4 produce a transcript product with a deletion of 213 bp that codified 9 amino acids of the intracellular domain, the entire transmembrane domain I, and the first 37 amino acids of the extracellular domain. According to the genomic organization that we proposed here, the third type of splicing occurred in P2X2-4 variant was the retention of the complete intron 11 (198 pb) that inserts 66 amino acids at the C-terminal region of the translated protein.

According with the model of Kawate et al (2009) and the secondary structure protein prediction program MEMSAT (Jones *et al.*, 1994), P2X2-4 subunit is predicted to be conformed by only one transmembrane domain, an extracellular N-terminal region and an intracellular C-terminal region (Jones *et al.*, 1994). P2X2-4 subunit, in the same way as P2X2-1 and P2X2-2, conserve the P2X2 consensus amino acids including the ten cysteines at the extracellular loop, the three consensus sites for N-linked glycosylation and the PKC phosphorylation site at the N-terminal (North, 2002).

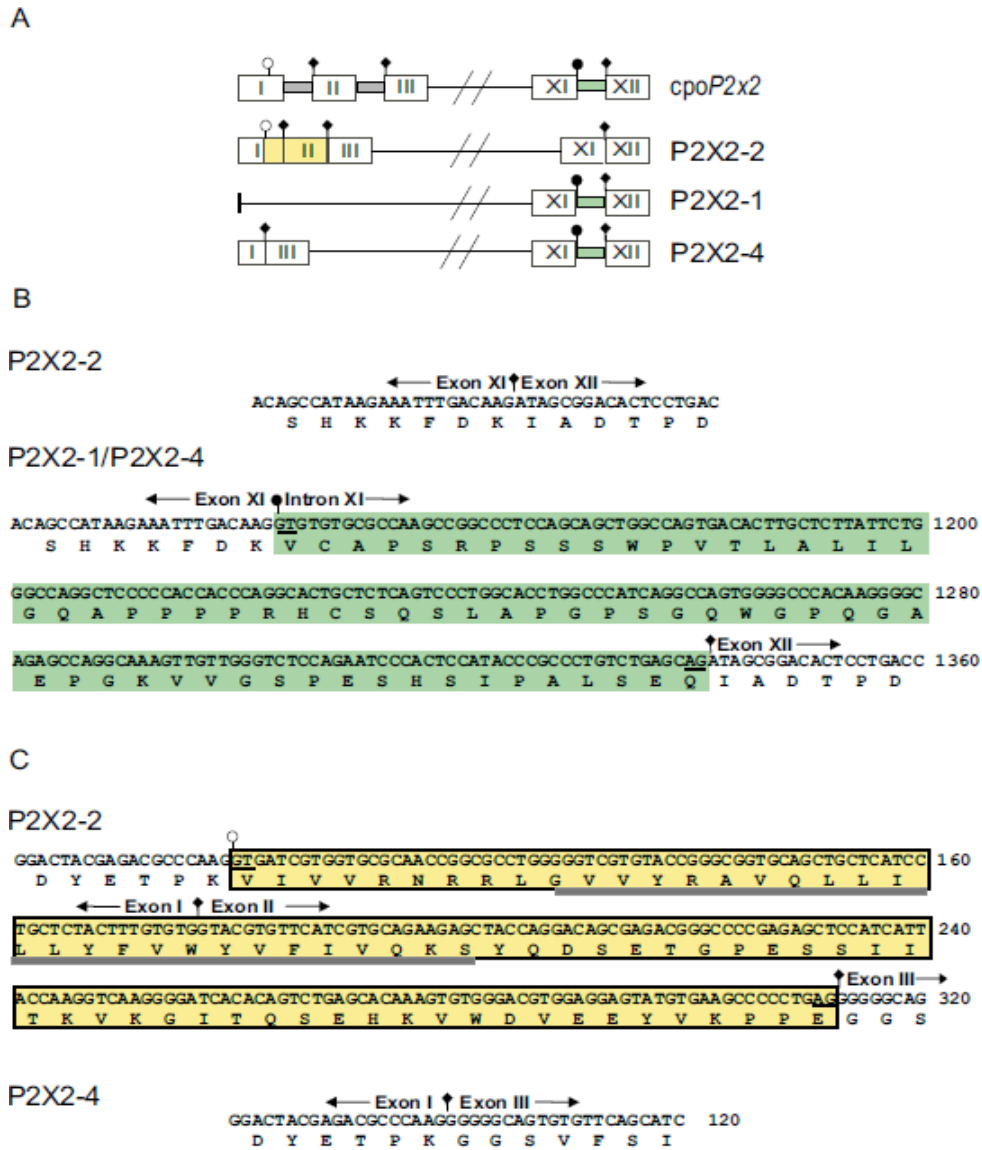


Figure 10. Schematic arrangements of the P2X2 splice variants found in intestine. **A)** Genomic organization of *P2x2* gene and mRNA of the fully processed variant (P2X2-1) and splice variants P2X2-1 and P2X2-4. Introns are shown as filled boxes and exons are represented as numbered boxes. For simplicity only segments from exons I to III and XI to XII are shown. Nucleotide and amino acid sequence of the segments showed in (A) are detailed in (B) and (C). **B)** The complete intron 11 is retained (green) in P2X2-1 and P2X2-4 splice variants, while is removed in the primary transcript P2X2-2. Consensus splice sites GT-AG are underlined. **C)** An alternative 5' splice site selection event in exon I (26 amino acids are lost), and exon II skipping (37 amino acids are lost), occurs in P2X2-4 splice variant. The yellow rectangle encloses the segments of exon I and II, absent in P2X2-4, compared to P2X2-2. Transmembrane domain I is indicated by a gray rectangle.

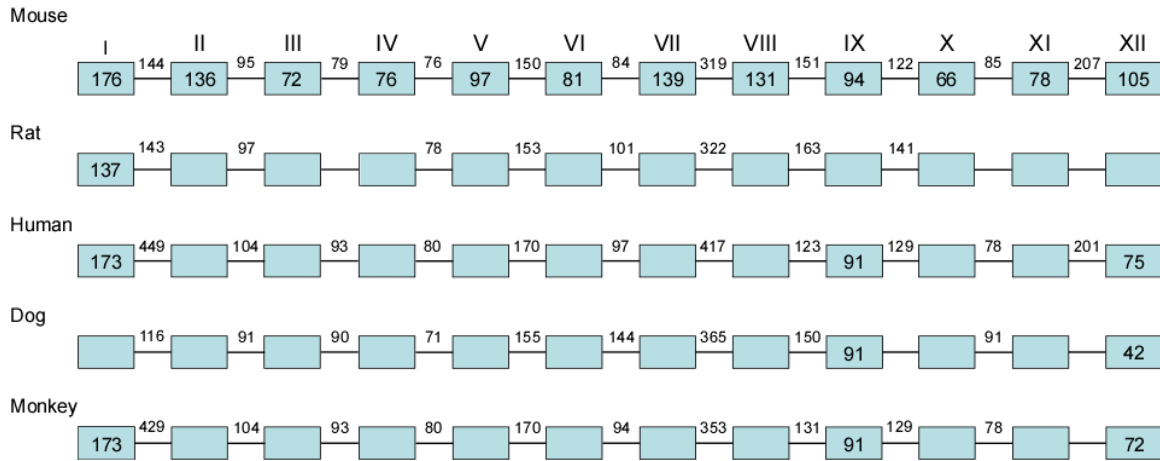


Figure 11. Proposed gene model of orthologous *P2x2* genes. Schematic representation of *P2x2* gene exon-intron organization for each species. The size of exons and introns are indicated in the mouse model, and when is not showed in the others species means that is identical to mouse.

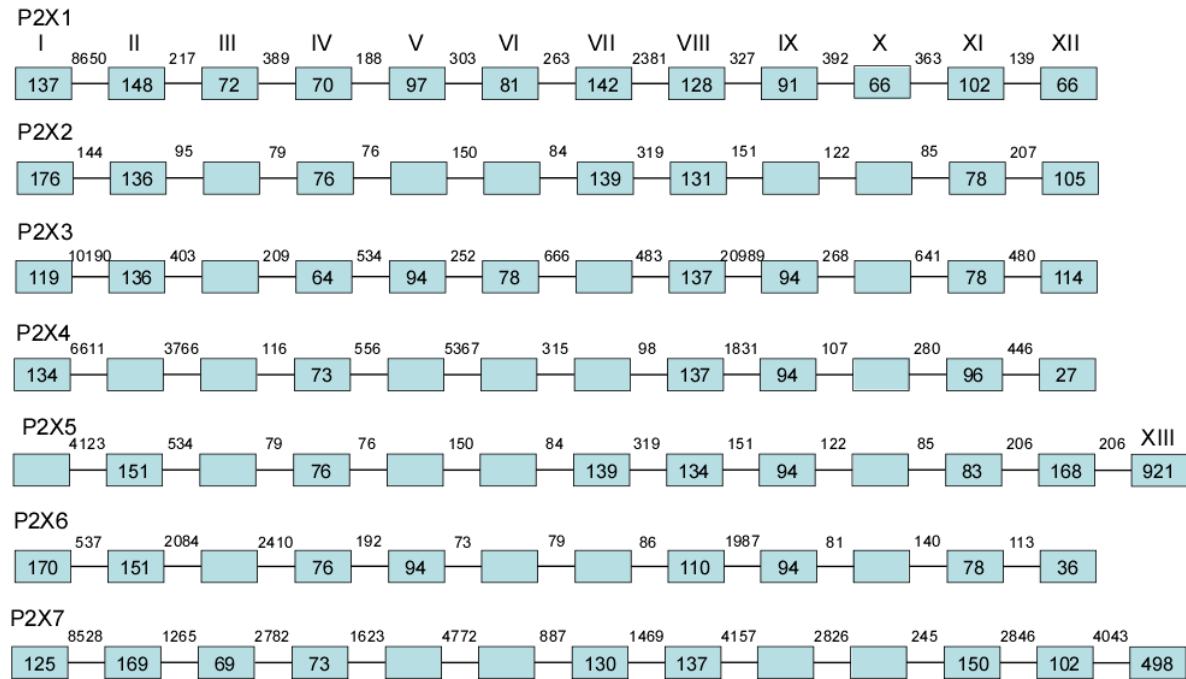


Figure 12. Genomic organization of *P2x* paralogue genes. Schematic representation of mouse *P2x* gene exon-intron organization. Mouse genes were taken as a reference because of the absence of genomic sequences of guinea pig *P2x* genes.

Identification of P2X2-1, P2X2-2, and P2X2-4 variants in single myenteric neurons by RT-PCR

To determine the presence of the P2X2 splice variants in the same cell, we used the first PCR reaction with external primers as a template to perform two semi-nested PCR reactions using specific primers to differentiate P2X2-1, P2X2-2, and P2X2-4 variants. The set of primers 1 distinguish by size P2X2-1 and P2X2-2 subunit, the set 2 distinguish P2X2-1 and P2X2-4 (see Materials and Methods). The P2X2 mRNA was detected in 92% (37 out of 40) of the myenteric neurons but the three splice variants were not found in all P2X2 positive cells. A representative example of four cells is shown in Figure 12A, and the distribution frequency for these receptors is shown in Figure 12B. P2X2-1 variant was found in the 37 positive cells, alone in 12 neurons (cell 3, Figure 12A and 12B) or together with other(s) P2X2 variants (n=25). Amplification of P2X2-1/2/4 was obtained in seven neurons (cell 1, Figure 12A and 12B), P2X2-1 with P2X2-4 in eight cells (cell 2, Figure 12A and 12B), and P2X2-1 with P2X2-2 in ten neurons (cell 4, Figure 12A and 12B).

Ionic currents mediated by P2X2 splice variants expressed in oocytes

ATP application evoked a fast inward current in oocytes expressing P2X2-1 and P2X2-2 (Figure 13) but not current was observed, even by high ATP concentrations (3 mM), in oocytes injected with P2X2-4 (no shown). In mouse, rat, and guinea pig, the most remarkable difference reported among P2X2 splice variants is the rate of desensitization. Here, we found similar findings. Thus, P2X2-1 desensitization was either slow or absent in

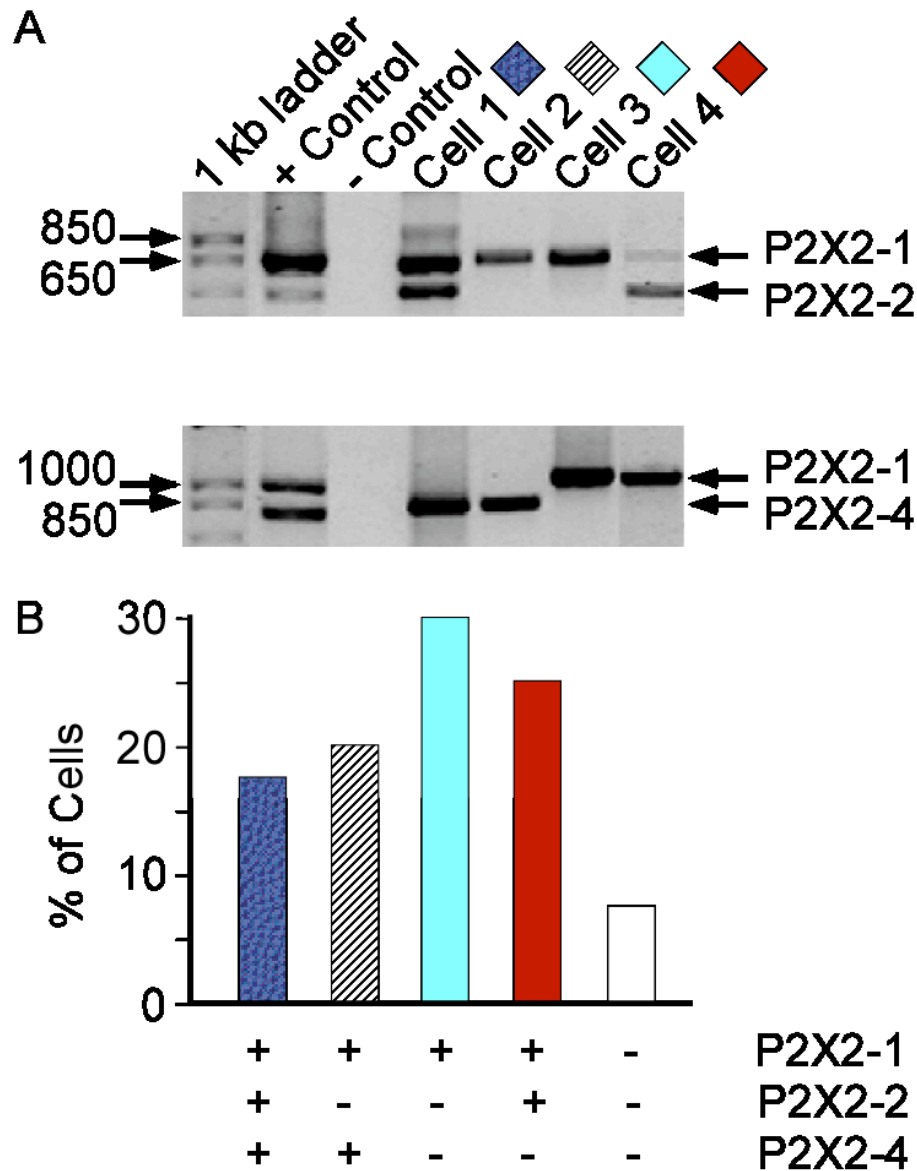


Figure 13. The P2X2 variants are distributed in different proportions in myenteric neurons, being P2X2-1 the most abundant transcript. **A)** Single cell RT-PCR performed with three sets of primers that distinguish P2X2-2 (set 1), P2X2-4 (set 2) or P2X2-1 (set 3) splice variants (see details in Materials and Methods) Representative agarose gel electrophoresis (1%) of four single neurons showing the presence of the three P2X2 variants (cell 1), P2X2-1 and P2X2-4 (cell 2), P2X2-1 (cell 3) and, P2X2-1 and P2X2-2 (cell 4). We used plasmid as positive control and negative control was done without template. **B)** Proportion (%) of individual myenteric neurons (n=40) showing the presence (+) and/or absence (-) of each P2X2 variant.

most oocytes. When a P2X2-1 desensitization was observed, it was well fitted to an exponential function with an estimated τ value of 300 ± 84 s (n=7), when an ATP concentration of $100 \mu\text{M}$ was

used. This slow desensitization kinetics was maintained even at 1 mM ATP concentration. The desensitization kinetics of currents through P2X2-2 channels was faster and less variable than that of P2X2-1. Thus, P2X2-2 receptor desensitization was well fitted by the sum of two exponentials functions ($\tau_1=6\pm0.4$ s and $\tau_2=75\pm9$ s, $n=11$), when an ATP concentration of 300 μ M was used, this concentration is equipotent to 100 μ M for P2X2-1 channels. Currents mediated by P2X2-1 had reproducible amplitudes during repetitive applications of the same concentration of ATP. However, the amplitude of the currents mediated by P2X2-2 receptors, in at least half of the recorded oocytes, were different to repetitive applications of the same ATP concentration. Data from experiments with no stable responses were discarded for further analysis.

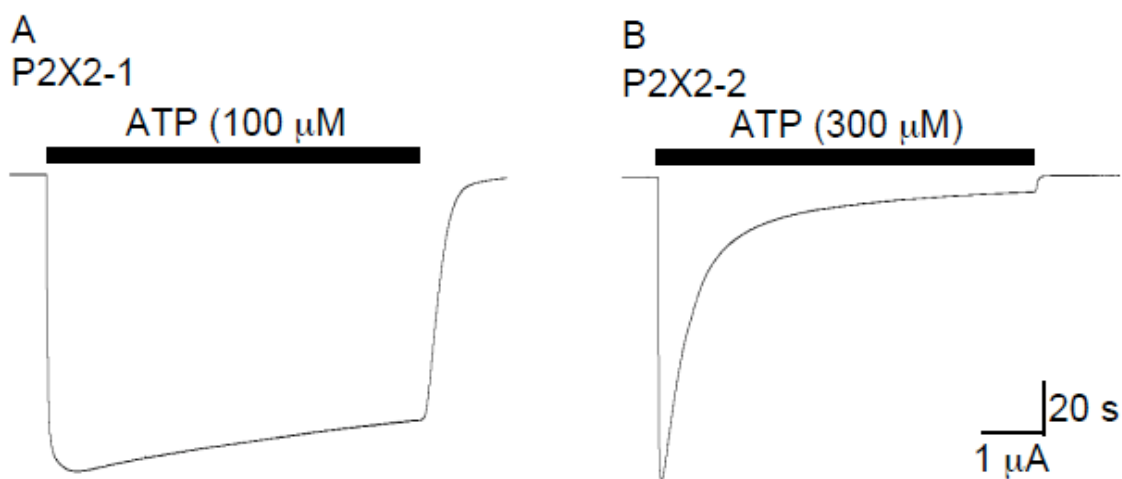


Figure 14. P2X2-1 and P2X2-2 form functional homomeric channels with different kinetics. Representative traces of ATP induced-currents recorded from *Xenopus laevis* oocytes expressing P2X2-1 (A) or P2X2-2 (B). Holding potential was -60 mV. Horizontal bars above traces indicate the ATP application, at 100 and 300 μ M that are equipotent concentrations.

In oocytes with stable responses, ATP (1-3000 μ M) induced currents in a concentration-dependent manner when P2X2-1 or P2X2-2 receptors were expressed (Figure 14A). Contrary to a previous report (Chen et al., 2000), we found these two P2X2 splice variants have different ATP sensitivity, being their EC_{50} values of 5.6 ± 0.9 (Hill coefficient 0.7 ± 0.07) and 17 ± 3 μ M (Hill coefficient

0.7±0.1) for P2X2-1 and P2X2-2, respectively. It has been well described that the ATP sensitivity of P2X2 receptors is dependent of the expression level (Clyne *et al.*, 2003; Fujiwara *et al.*, 2004), to avoid this problem we only recorded cells with maximal ATP responses lower than 10 μ A. Indeed, we showed virtually the same EC₅₀s for the different magnitudes of currents that we recorded in this study (Figure 14B), which rules out the possibility that the different ATP affinity displayed for both P2X2 variants were due to a difference in their expression levels. We tested the effect of other agonists in order to determine if this difference was also evident.

2'-3'-O-(4-benzoylbenzoyl)-ATP (BzATP) also activated channels formed by either P2X2 variant with an efficacy much lower than ATP (Figure 14C). On P2X2-1 receptors, BzATP (0.3-100 μ M) had a similar potency than ATP (EC₅₀ value of 4.4±2 μ M) and its efficacy was only 40% of the maximal response induced by 1 mM ATP. On P2X2-2 receptors, BzATP (3-1000 μ M) potency (EC₅₀ >100 μ M) was lower than that of ATP. Its efficacy (>50%) appears to be higher than on P2X2-1 receptors, although, the EC₅₀ and efficacy values could not be calculated with precision because the maximal response was not reached (Figure 14B). Therefore, we compare the effect of a single BzATP concentration on both channels and we obtained significant differences (p<0.05) that were of 22±7 (n=5) and 3.2±1.8% (n=4) with BzATP 3 μ M, and 41±9 (n=4) and 14±4% (n=4) with BzATP 30 μ M, for P2X2-1 and P2X2-2, respectively.

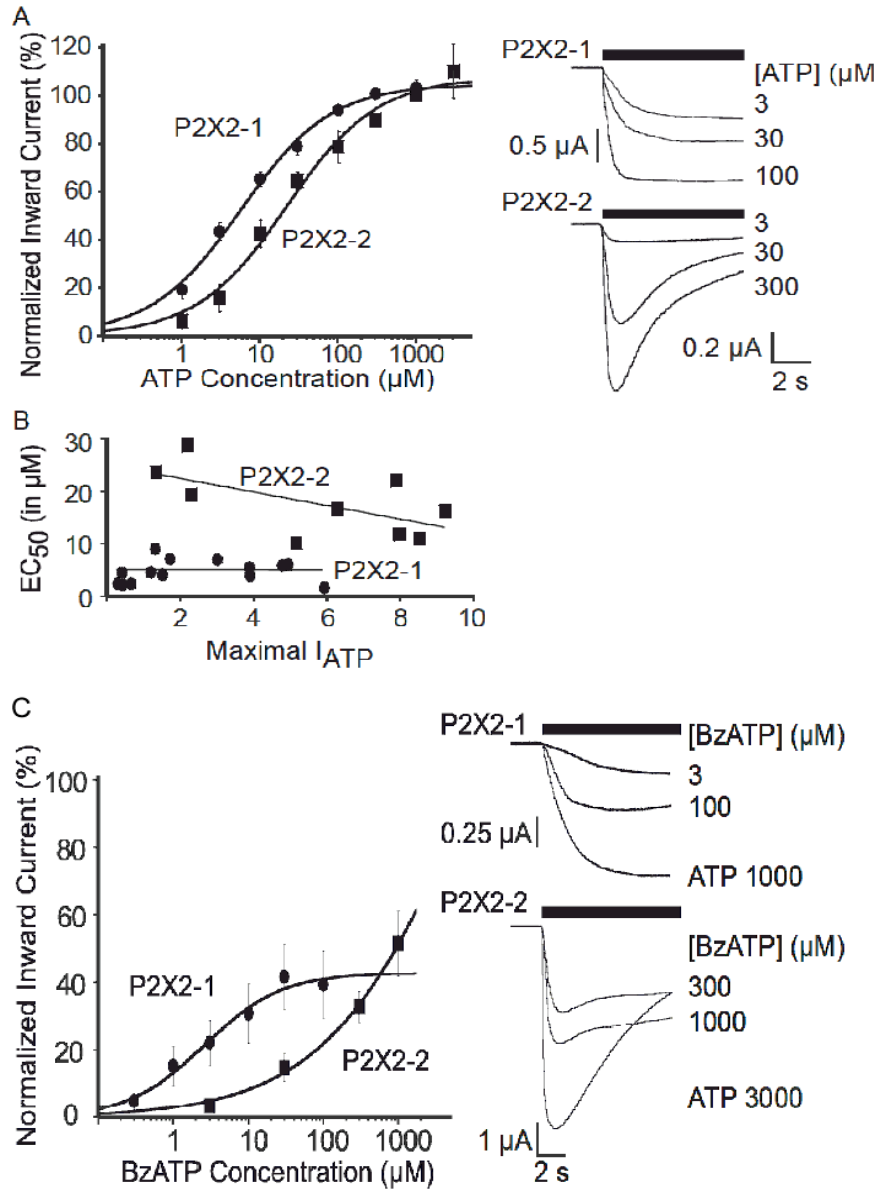


Figure 15. P2X2 splice variants have different sensitivity to ATP and BZATP. **A)** Concentration-response curves for ATP to activate membrane currents mediated by P2X2-1 or P2X2-2 receptors. Data are well fitted with a logistic equation; each symbol represents the average value of four to thirteen experiments for P2X2-1 and six to sixteen for P2X2-2. **B)** Correlation between the expression level in individual cells and the maximal response to ATP for both P2X2-1 and P2X2-2 variants. **C)** Concentration-response curves for BzATP to activate membrane currents mediated by both P2X2 receptors variants. Symbols represent average data of three to seven experiments for P2X2-1 and four to five for P2X2-2. For both agonists, responses were normalized using as 100% the current induced by equipotent ATP concentrations, 1 for P2X2-1 and 3 mM for P2X2-2. Vertical lines associated with symbols are S.E.M of relative currents. Current traces from representative experiments are shown to the right of both graphs.

α,β -meATP (100 μ M) induced only a marginal response on both P2X2-1 ($7\pm 1.6\%$) and P2X2-2 ($6.7\pm 3.5\%$; Figure 15) compared against ATP. Co-application of ATP with α,β -meATP (100 μ M of each) in P2X2-1 receptors showed a reduction in the I_{ATP} of $22\pm 7\%$ (Figure 15A; $n=3$), but no effect was seen in P2X2-2 channels (Figure 15B; $n=4$). In the last experiments we used quasi-maximal concentrations of ATP to activate P2X2-1 (100 μ M) and P2X2-2 (1 mM).

Effects of antagonist on P2X2 splice variants

For these studies, we tested the effects of the different antagonists on I_{ATP} induced by equipotent concentrations of ATP, for instance, because we observed low I_{ATP} inhibition using high ATP concentration (6.5% with ATP 1 mM plus suramin 100 μ M for P2X2-1), therefore, we tested the effect of suramin using 30 μ M and 100 μ M ATP on P2X2-1 and P2X2-2, respectively. Suramin inhibit both splice variants of the P2X2 receptor in a concentration-dependent manner, with one major difference, its effect on P2X2-1 is clearly biphasic (Figure 16) and monophasic on P2X2-2 (Figure 17). On P2X2-1, the first phase is seen at concentrations lower or equal than 10 μ M (with an IC_{50} of 0.4 μ M). The second phase was seen at above 30 μ M, with an IC_{50} of 486 μ M. These two IC_{50} values were calculated from means shown in Figure 16C. The maximal inhibition for the first phase was about 19%. On P2X2-2 receptors, suramin has not effects at low concentrations (<10 μ M, see Figure 17). Suramin inhibition occurs at concentrations equal and higher than 30 μ M, being the IC_{50} of 203 (Figure 17C). Suramin effects on both P2X2 receptors were reversible 3 min after its wash out (Figures 16 and 17). A possible explanation for the different suramin effects observed on the two variants is that the two binding sites of P2X2-1 are also present in P2X2-2 but

in this channel these binding sites have a closer suramin affinity, which would complicate the separation of the inhibitory effects mediated for these sites. In agreement with this interpretation, the suramin IC_{50} on P2X2-2 receptors has a value between those determined for both inhibitory phases of P2X2-1

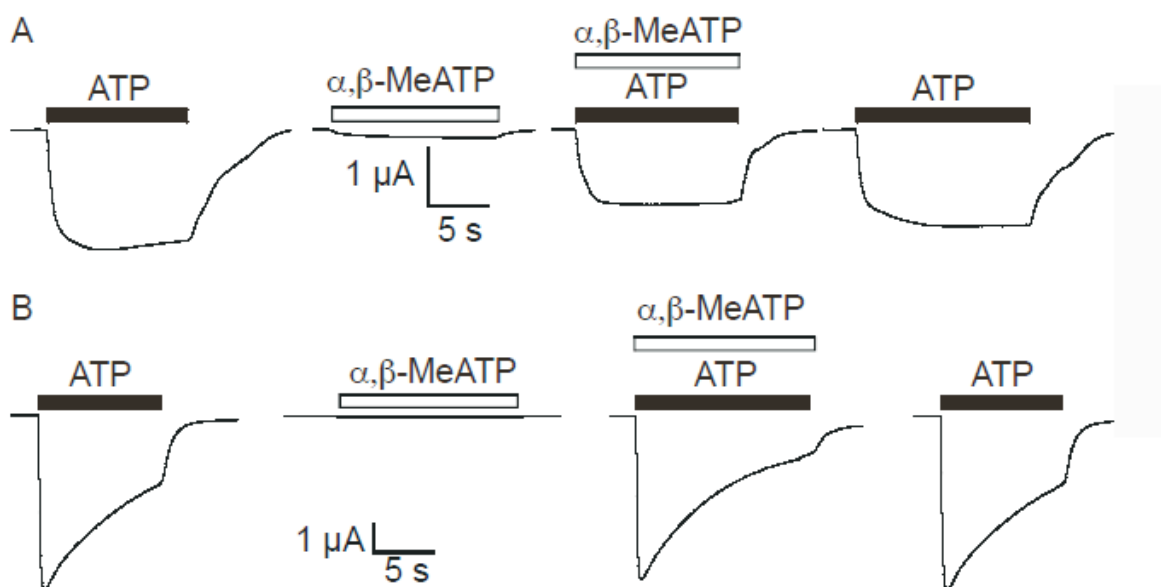


Figure 16. α,β -meATP activates both P2X2 receptor variants with very low potency but behaves as an antagonist only at P2X2-1 receptors. The first two traces in **(A)** (P2X2-1) and **(B)** (P2X2-2), are representative recordings of the currents induced by ATP (I_{ATP}) or α,β -meATP (100 μ M). The inhibitory effect of the last nucleotide on I_{ATP} is also shown by co-application of both agonists, α,β -meATP inhibits only P2X2-1 channels (A). The right most trace was taken 3 min after the washing out of α,β -meATP. For these experiments we used quasi-maximal concentrations of ATP to activate P2X2-1 (100 μ M) and P2X2-2 (1 mM).

In a previous study (Chen *et al.*, 2000), suramin (100 μ M) was shown to be inactive on P2X2-1 but inhibited the P2X2-2 receptor when these were activated with 10 μ M ATP, unfortunately in that study concentrations-response curves were not carried out. Here we tested the effect of suramin (100 μ M) on responses induced by 10 and 30 μ M of ATP (equipotent concentrations) on P2X2-1 and P2X2-2 channels and we found a substantial inhibition of both channels, 56 ± 10 (n=5) and

68±1 % (n=3), respectively. This demonstrates that suramin inhibitory effect described here is not due to the different concentrations of ATP used here and previously (Chen *et al.*, 2000).

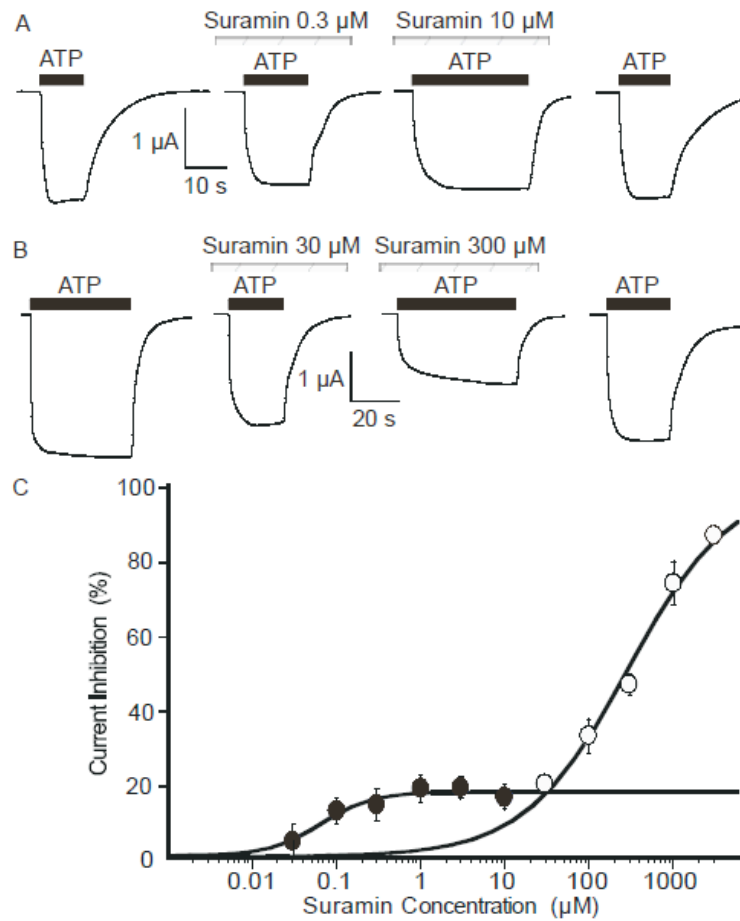


Figure 17. Suramin inhibits P2X2-1 receptors in a biphasic-manner. **A)** and **B)** are representative traces of the currents induced by ATP (I_{ATP} ; 30 μ M) before, in the presence, and after application of suramin, at low (**A**) and high (**B**) concentrations. **C)** Concentration-response curve of the effects of suramin on I_{ATP} (30 μ M). Two inhibitory phases are evident. Lines are the best fittings to a logist function of the data between 0.03 to 10 μ M (closed symbols) and between 30 to 3000 μ M (open symbols) of suramin. Estimated IC_{50} s for these two phases were 0.07 ± 0.02 and 286 ± 32 μ M, respectively. For the fitting of the second phase we assumed 100% inhibition. Each symbol represents the average value of four to six experiments.

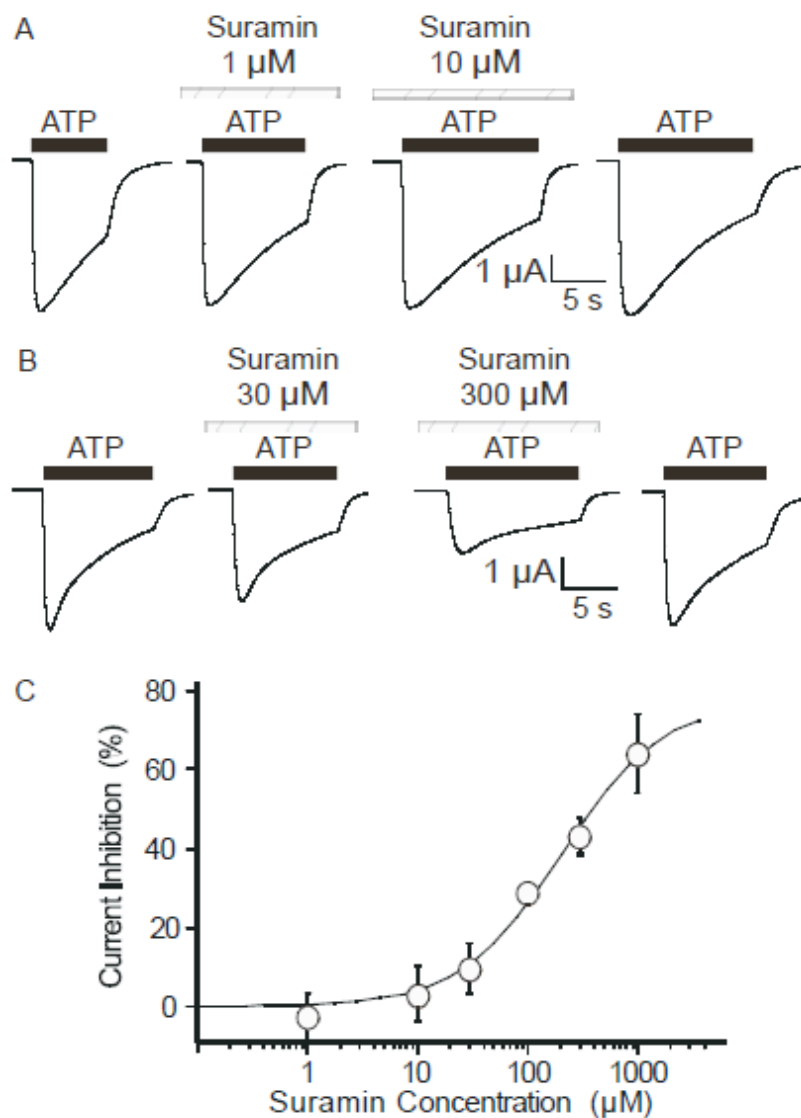


Figure 18. Suramin inhibits P2X2-2 receptors in a monophasic-manner and only at high concentrations. **A)** and **B)** show representative traces of the currents induced by ATP (I_{ATP} ; 100 μ M) before, in the presence, and after application of suramin, at low (**A**) and high (**B**) concentrations. **C)** Concentration-response curve of suramin on I_{ATP} mediated by P2X2-2 channels. Estimated IC_{50} was 204 ± 83 μ M. Each symbol represents the average value of three to six experiments.

PPADS inhibitory effect was previously investigated on P2X2-1 and P2X2-2 receptors from the guinea pig cochlea; however, it was done using a single concentration of PPADS (100 μ M) and before reaching the steady state of this antagonist (Chen *et al.*, 2000), which is quite relevant because PPADS is

known to slowly bind to P2X receptors (Barajas-Lopez *et al.*, 2000; Barajas-Lopez *et al.*, 1996a). Therefore, here we pre-apply this antagonist for 4 min before testing its effects on I_{ATP} . We found that PPADS also inhibited both receptors in a concentration-dependent manner (Figure 18). However, its effect was more potent on P2X2-1 than P2X2-2 ($P \leq 0.05$) with IC_{50} s of 0.8 ± 0.2 (Hill coefficient 1.1) and 2.4 ± 0.5 μ M (Hill coefficient 1.1), respectively. PPADS effects on both P2X2 receptors were reverted 3 to 10 min after its wash out, depending of its concentration. For these experiments, P2X2-1 and P2X2-2 receptors were activated with equipotent concentrations of ATP, 1 and 3 mM, respectively.

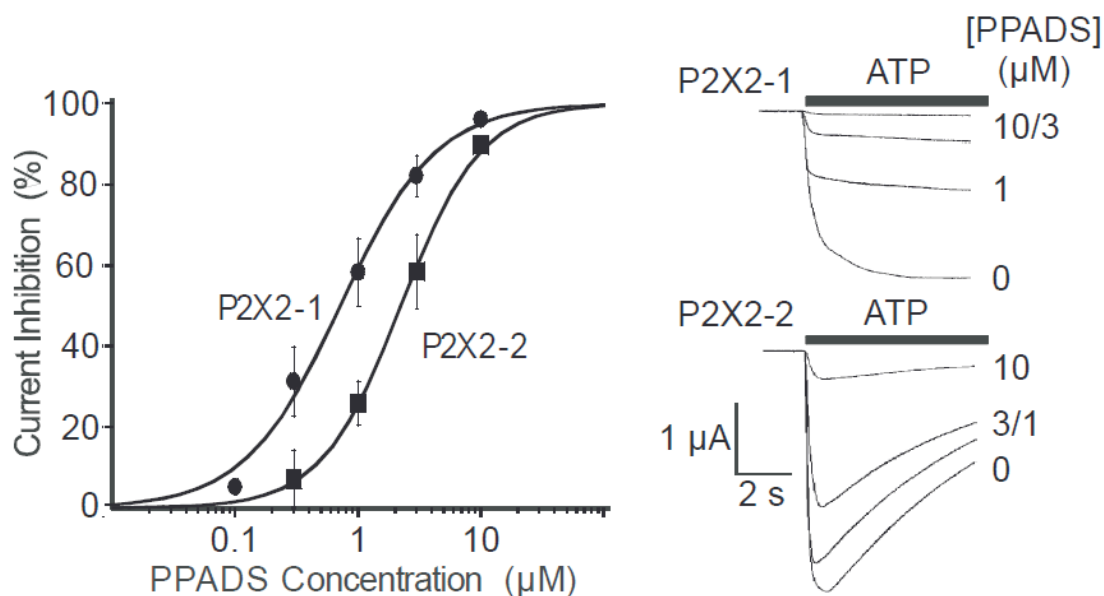


Figure 18. PPADS is clearly more potent on P2X2-1 than on P2X2-2 receptors. Concentration-response curves for the inhibitory effect of PPADS on ATP induced currents (I_{ATP}). Equipotent concentrations of this nucleotide were used to activate P2X2-1 (1 mM) and P2X2-2 (3 mM) receptors. PPADS was pre-applied during 4 min before measuring the ATP responses. In the graph, each symbol represents the average value of three to six experiments for P2X2-1 and four experiments for P2X2-2. Using these mean values the estimated IC_{50} s were 0.8 μ M (P2X2-1) and 2.3 μ M (P2X2-2). Current traces from typical experiments are shown to the right.

Table 4. Properties of P2X2-1 and P2X2-2 receptors expressed in *Xenopus laevis* oocytes.

Receptor	Tau of desensitization (seconds)	Agonists EC ₅₀ (μM)			Antagonists IC ₅₀ (μM)			
		ATP	BzATP	α,β-MeATP	Suramin	PPADS	Zinc	α,β-MeATP
P2X2-1	τ ₁ = 300±84	6±0.7	2.6±1	>100	0.07±0.02 286±32	0.7±0.06	250±34	>100
P2X2-2	τ ₁ = 6±0.4 τ ₂ = 75±9	22±5	>100 μM	>100	204±83	2±0.08	485±30	Inactive

DISCUSSION

Here, we reported the cloning of three variants of P2X2 receptor from the guinea pig intestine, which were also shown to be present in single myenteric neurons. P2X2-1 and P2X2-2 variants form functional homomeric channels when were expressed in *Xenopus* oocytes. The third variant, P2X2-4, did not form functional channels. Based on analysis of the structural organization of these variants it was predicted that P2X2-2 was the main isoform, which lead us to propose here a new arrangement in the *P2x2* gene consisting of 12 exons and 11 introns. In agreement with this new model, intron 11 is retained in P2X2-1 variant by alternative splicing, which is responsible of significant phenotypical changes in the current kinetics and pharmacological properties of this receptor.

The difference in the ATP EC₅₀s values between both P2X2 variants we report here differ those previously reported. Under similar experimental conditions, in mice the shorter form of this receptor (P2X2-2) exhibits an ATP-sensitivity similar to P2X2-1 (the longer version) (Koshimizu *et al.*, 2006; Koshimizu *et al.*, 1998). In the guinea pig, however, we found that the shorter form had lower sensitivity to ATP (P2X2-2) and BzATP than P2X2-1 (Table 4). As in other species (Evans *et al.*, 1995; Lynch *et al.*, 1999), BzATP also behaved as a partial agonist for P2X2 receptors. Contrary to our findings, Chen *et al.* (2000) report that P2X2-1 and P2X2-2 variants from the guinea pig had a very similar agonist profile. However, these authors did not carry out full concentration-response curves and the effect of BzATP was not tested. Although some reports have showed that the expression level of P2X2-1 channels changes the ATP EC₅₀ and others properties (Clyne *et al.*, 2003; Fujiwara *et al.*, 2004), we demonstrated that expression level doesn't explain the differences we have seen here. Additionally, we report an even larger pharmacological difference with the agonist BZATP, thus P2X2-1 was quite sensitive to this

agonist, with an EC₅₀ of 4 μM, similar to the reported before (Coddou *et al.*, 2011). P2X2-2 was far less sensitive (EC₅₀>100 μM) BZATP, which indicates that this agonist can be used to study the role of both variants in native cells.

P2X2-1 and P2X2-2 channels had also a different antagonist profile. Thus, the former was more sensitive to PPADS and Zn²⁺ than the P2X2-2 receptor. Suramin inhibited both variants but in a biphasic- and monophasic-manner, respectively. α,β-meATP was more effective to inhibited P2X2-1 than P2X2-2 channels. A previous study (Chen *et al.*, 2000), reports that these two P2X2 isoforms from the guinea pig have similar antagonist profile, only suramin appears to inhibit more the P2X2-2 than P2X2-1 channels. However, observations of these authors are based on application of a single antagonist concentration, which makes uncertain any comparison with the data described here.

The physiological relevance of the splice variants for P2X2 murine (Koshimizu *et al.*, 2006) and rat (Brandle *et al.*, 1997; Simon *et al.*, 1997) receptors has been well documented. Thus, in these rodents, the shorter forms of this receptor desensitized more rapidly than the longer version, which was not observed with the human receptor variants (Lynch *et al.*, 1999). In the guinea pig cochlea, a previous study (Chen *et al.*, 2000) reported faster desensitization kinetics for P2X2-1 (τ₁=3.9 and τ₂=15.8 s) and P2X2-2 (τ₁=1 and τ₂=7.6 s) than those reported here (Table 2). These discrepancies may result from the different expression systems used (HEK293 cells and *Xenopus laevis* oocytes) (Koshimizu *et al.*, 2006) and/or from the sequence differences of the P2X2 isoforms reported here to those previously reported (Parker *et al.*, 1998). Indeed, the versions of P2X2 previously reported (Parker *et al.*, 1998) have nucleotide changes, and insertions absent in the guinea pig genomic P2X2 sequence, which modified the amino acid sequence (Annex 1). Our hypothesis is that these sequence changes are responsible for the functional differences

observed between our group and Chen *et al* (2000) regarding the functional and pharmacological properties of P2X2-1 and P2X2-2 receptor variants.

Current P2X receptor model indicates that agonists and antagonists would bind to their extracellular domain. Indeed, recent structural data obtained from the crystal structure of zebrafish P2X4 receptor (Kawate *et al.*, 2009), indicates that ATP and its analogs likely bind to a non-canonical site $\sim 45\text{\AA}$ from the ion channel at the extracellular domain and very close to this site would bind antagonists and divalent cations. It has also been shown that various positive residues situated at the ectodomain are likely important to the inhibitory effect of suramin (K138 in human P2X1), PPADS (K246 in rat P2X2), and for the modulatory effects of Zn^{2+} (H120 and H231 in rat P2X2; (see Buell *et al.*, 1996; Sim *et al.*, 2008; Tittle *et al.*, 2008). Here we report two P2X2 isoforms that are identical at their extracellular loop and them, however, had distinct pharmacological properties, indicating that structural changes at this loop must be occurring by insertion of the 66 amino acids at the C-terminal domain. A similar finding was reported by Pan *et al* (2005), they found that the mMOR-1B4 splice variant of the μ -Opioid receptor that has modifications at the amino acid sequence of the C terminus far from the agonist binding site, influence the binding characteristics, efficacy, and potency of μ -Opioids (Pan *et al.*, 2005)

One possibility to explain our findings is that a larger C-terminal domain might allow interactions with cytoplasmic structures and this would originate structural changes in the extracellular domain of the receptor, increasing the sensitivity of P2X2-1 receptors to agonist and antagonist. In support to this idea, interactions of the scaffolding protein Fe65 and tubulin with the P2X2-1 receptor were reported using yeast 2-hybrid analysis (Guimaraes, 2008; Masin *et al.*, 2006). Regulatory motifs inside intron XI appear to be involved in such interactions, being proline rich regions the probable binding site for Fe65, and the 378-397 amino acids of P2X2-1 the binding site for β -tubulin I. Additionally, there are highly potential phosphorylations sites included

at this region (385S, 386S, 387S, 431S and 436S as predicted with NetPhos program: <http://www.cbs.dtu.dk/services/NetPhos/>) (Blom *et al.*, 1999) that could be also implicated in regulatory functions in P2X2 channels.

We also found the expression of a truncated P2X2 subunit (P2X2-4), lacking part of the N-terminal, ectodomain and the entire TM1 (see Figure 9) of unknown function that failed to respond to ATP. Similar subunits have been reported in P2X channels and was suggested that interactions of this truncated and apparently no functional subunits is a mechanism of receptor regulation. A P2X7 receptor lacking the entire C-terminus, TM2 and the distal third part of the extracellular loop was capable to form heteromeric receptors with the full length P2X7 subunit and mediate apoptosis (Feng *et al.*, 2006). Several truncated P2X2 splice variants have been found in human and rat, however their functional role are still unknown (Table 2). Even though P2X2-4 subunit was apparently no functional, we found this truncated isoform co-expressed with any of the others two variants in 37% of the neurons tested, suggesting a possible modulatory role of P2X2-4 subunit in myenteric neurons. It remains to be investigated if this subunit is capable to assemble and form heteromeric receptors.

P2X native receptors that show high ATP-sensitivity are expressed in about 90% of myenteric neurons (Barajas-Lopez *et al.*, 1996a; Galligan *et al.*, 1994), which share various pharmacological properties that better resemble those described here for the recombinant P2X2-2 receptor variants. Thus: i) they have similar sensitivity to ATP, BzATP, and α,β -meATP (Valdez-Morales *et al.*, 2011); ii) BzATP behaves as a partial agonist on them (Valdez-Morales *et al.*, 2011); iii) they are sensitive to PPADS; and iv) the desensitization kinetics of the P2X2-2 receptor variant (Table 4) is similar to that of P2X native receptors ($\tau_1=5.7$ and $\tau_2=121$ s; (Barajas-Lopez *et al.*, 2002)). A striking difference, however, is that the suramin inhibits P2X2-2 but it has a double

effect on native myenteric neurons, always potentiates but also frequently inhibits I_{ATP} at concentrations $\geq 100 \mu\text{M}$ (Guerrero-Alba *et al.*, 2010). Suramin effects would indicate that native myenteric P2X channels, with high ATP-sensitivity (Valdez-Morales *et al.*, 2011) are most likely heteromeric, formed by the combination of P2X2 receptor variants with other subunits. This hypothesis is further supported by the fact that P2X2-2 subunit appears to be present only in 43% of myenteric neurons and the properties of native channels are clearly different than those reported here for the P2X2-1 isoform, the most common variant. Currently, we are exploring the possibility of hetero-trimeric assembly of both P2X2 isoforms with other P2X2 receptors found in myenteric neurons in order to better understand their functional roles. With the same purpose, we need to investigate in future studies the distribution and properties of P2X receptors in the myenteric neurons of other species and organs and during different physiological and pathophysiological conditions.

The percentage of myenteric neurons expressing P2X2 mRNA (92%; present study) correlates well with the percentage of myenteric neurons expressing functional P2X channels (>90%) (Guerrero-Alba *et al.*, 2010; Valdez-Morales *et al.*, 2011). However, strong immunoreactivity for P2X2 receptor was seen in only 30% of the myenteric neurons (Castelucci *et al.*, 2002), which indicates that the used antibody mainly detects one of the P2X2 isoforms. The antibody (AB5244, Chemicon) used by Castelucci *et al.* (2002) is directed against the last amino acids of the C-terminal domain, and it is possible that the 66 aa introduced (in variant P2X2-1 and P2X2-4) could decreased receptor immunoreactivity and this could be responsible of the weak immunoreactive subpopulation of myenteric neurons (Castelucci *et al.*, 2002). However, based on the distribution of the variants and the strong immunoreactivity observed it is more likely that the antibody is reacting against the P2X2-2 isoform. In support to this idea, the P2X2-2 variant was

detected in only 43% whereas P2X2-1 (with or without P2X2-4) was in the great majority (92%) of myenteric neurons.

Various aspects remain to be solved in order to better understand the role and contribution of P2X2 splice variants to the I_{ATP} in myenteric neurons. During my doctoral thesis I did additional experiments that provided us with important preliminary data about two issues. First, we demonstrated that P2X2 splice variants, when coexpressed in oocytes, can coassemble to form heteromeric channels, as it is shown by the fact that I_{ATP} of these experiments have very different kinetics than the homomeric channels along or than the predicted currents resulted of the additive contribution of P2X2-1 and P2X2-2 homomeric channels (Figure A.1). However, two heteromeric channel populations appear to be generated, one of them with a much higher sensitivity to ATP than the other (Figure A.2), although, both channels populations maintained the same desensitization kinetics. A simple explanation for these observations is that heteromeric channels with higher ATP sensitivity are composed by two P2X2-1 subunits and one P2X2-2GQ, and those with lower sensitivity are formed by two P2X2-2GQ subunits and one P2X2-1. These observations would imply that activation of two subunits is enough to open P2X channel and that the presence of at least one subunit is sufficient to modify the desensitization process, because both possible stoichiometric arrangements have the same kinetics.

CONCLUSION

In conclusion, we cloned three P2X2 receptor variants from the guinea pig intestine, which we identified in single myenteric neurons. P2X2-1 and P2X2-2 variants form functional homomeric channels but not the P2X2-4 variant. The analysis of the structural organization of the variants indicates that the fully processed isoform is P2X2-2, which leads us to propose a new exon-intron arrangement in the *P2x2* receptor gene consisting of 12 exons and 11 introns. Intron 11 would be retained in P2X2-1 and P2X2-4 variants by alternative splicing. The P2X2-1 is the most common

P2X2 variant present in myenteric neurons and displays significant phenotypical changes in its current kinetics and pharmacological properties indicating that retention of the intron 11 has an important role in ATP signaling in the myenteric plexus of the small intestine.

APPENDIX A

**P2X2 receptors variants form heteromeric channels with
different stoichiometry**

INTRODUCTION

Many aspects remains to be resolved about the role of P2X2 splice variants and their contribution to the I_{ATP} in myenteric neurons. Some unresolved questions are: Could these subunits coassemble in heteromeric channels conformed of P2X2 splice variants or others P2X subunits? What would be their functional and pharmacological properties? What is their stoichiometry these P2X2 isoforms in native cells? How P2X2 splice variants contribute to the ATP response in myenteric neurons? What is the role of P2X2-4 splice variant?. In attempt to resolve some of these questions we performed some preliminary experiments in which we coexpressed P2X2-1 and P2X2-2 subunits and characterize their pharmacological and biophysics properties. Our data indicate that heteromeric channels with two different stoichiometries are formed.

METHODS

We used the same protocols and equipment described in the Section of Methods. One difference however, is that here we injected in *Xenopus* oocytes mRNA of P2X2-1 variant and of a mutated version of P2X2-2 (P2X2-2GQ) that has a fastest desensitization kinetics and lower ATP sensitivity, with the idea that these characteristics would allow us to better differentiate possible homomeric from heteromeric channels.

RESULTS

As shown in Figure 19 the desensitization kinetics of coexpressing cells was adjusted to one exponential, suggesting that there is a homogenous population of heteromeric receptors. Furthermore, desensitization was clearly different to the expected if independent homomeric assembly of P2X-1 and P2X2-2GQ occurred. At the moment two batches of oocytes from different frogs were tested and desensitization kinetics were similar in all cells. However, different ATP

potency was observed between these two oocytes batches. As it is shown in Figure A.2A, oocytes from one batch displayed an EC_{50} similar to P2X2-1 homomeric channels (7 μ M) and those of the second batch had an EC_{50} similar to P2X2-2GQ homomeric channels (116 μ M). These findings indicate that heteromeric assembly of both isoforms occurred with different stoichiometry.

DISCUSSION

We proposed that channels with higher ATP sensitivity are composed by two P2X2-1 subunits and one P2X2-2GQ, and those with lower sensitivity are formed by two P2X2-2GQ subunits and one P2X2-1. This would imply that activation of two subunits is enough to open P2X channels. Furthermore, our data also imply that the presence of at least one subunit is sufficient to modify the desensitization process because both possible stoichiometric arrangements have the same kinetics.

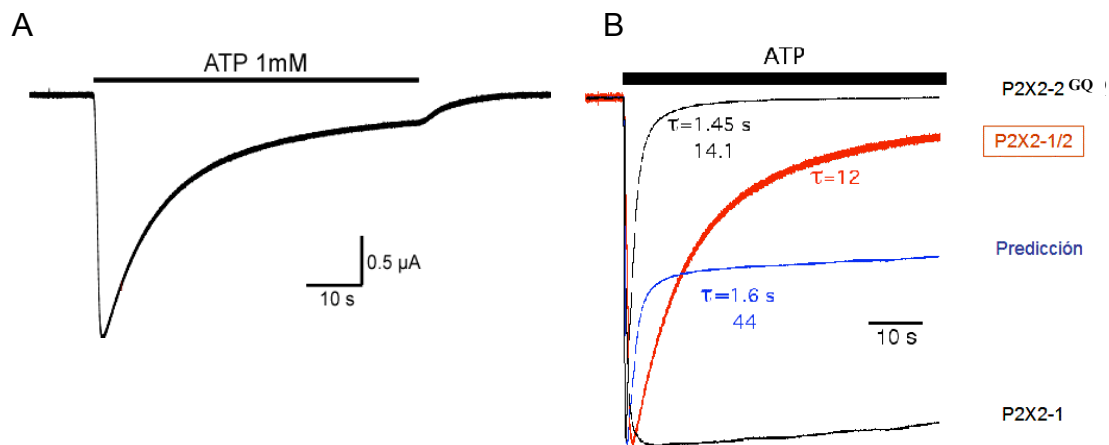


Figure A.1. Desensitization kinetics in *Xenopus* oocytes coexpressing P2X2-1/P2X2-2GQ suggests the formation of heteromeric channels. **A)** Representative recording of the I_{ATP} from *Xenopus* oocytes coinjected with P2X2-1 and P2X2-GQ mRNAs. **B)** ATP application induces inward currents with a desensitization kinetics that is quite different to the predicted if both subunits were forming independent homomeric channels. Estimated τ values are indicated in each case. P2X2-2GQ correspond to the mutated version of P2X2-2 containing E26G and L185Q changes at the N-terminal and extracellular domain, respectively.

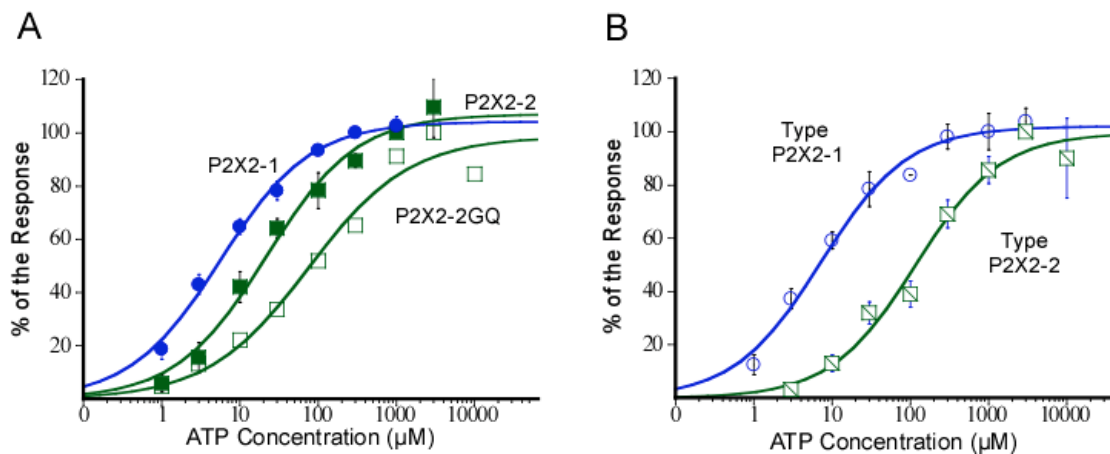


Figure A.2. Coexpressed P2X2-1/P2X2-2GQ subunits showed to types of ATP response. **A)** Control concentration-response curves for ATP to activate currents mediated by homomeric channels: the mutant P2X2-1GQ (empty squares; $EC_{50} = 76 \pm 37 \mu M$), the wild P2X2-2 (filled squares) and the wild P2X2-1 (circles). **B)** Concentration-response curves for ATP from oocytes coexpressing P2X2-1 and P2X2-2GQ subunits. Two types of batches of oocytes were distinguished: one showing ATP sensitivity like P2X2-1 ($EC_{50} = 7 \pm 1 \mu M$), and other like P2X2-2GQ ($EC_{50} = 116 \pm 36 \mu M$).

APPENDIX B

Characterization of myenteric P2X₂ variants from mouse

INTRODUCTION

Previously data from our laboratory has shown that native guinea pig and murine myenteric P2X display different pharmacological properties. In guinea pig, suramin has inhibitory and potentiatory effects on these receptors. In murine receptors, suramin inhibited the IATP whereas in guinea pig suramin has inhibitory and potentiatory effects that are mediated by two different binding sites (Guerrero-Alba *et al.*, 2010). Therefore, these observations suggested the existence of different populations of P2X receptors (with others P2X subunits and/or splice variants) in mouse and guinea pig neurons. In order to explore the possibility that mouse and guinea pig P2X2 splice variants were different, we cloned and characterized the mouse P2X2 variants. Because several reports indicate that specific pharmacological differences are observed between P2X of different species, we also investigate the pharmacological properties of murine P2X2 receptor we isolated.

MATERIALS AND METHODS

Cloning of P2X2 and single cell PCR

The strategy used was similar to the described before. Briefly, Total mRNA was extracted from mouse intestine and cDNA was synthesized using the Super SMART cDNA synthesis technique (Clontech) following the manufacturer's specifications. PCR was performed with specific primers (F: 5'CTTGTGGACCGAGCTCCTTG'3, R: 5' CGTGGACATGGTTACTGAAGAGC'3) to amplify the entire ORF of mouse P2X2 subunit using Platinum Taq DNA Polymerase (Life Technologies, Texas, USA). We used 40 round of amplification with an aligning temperature of 64°C. The fragments were cloned and sequenced.

For single cell PCR, neurons were cultivated and harvested with the same protocol as guinea pig. For the first PCR reaction we used the external primers mentioned above and for nested PCR we combined the same forward primer with the reverse 5' CCGATGGAGGTCAGAGCAGTG'3. A total of 70 round of amplification (35 for each PCR protocol) were performed.

Pharmacological characterization in Xenopus oocytes.

Oocytes were injected with 0.4 or 0.8 ng of mRNA. Concentration-response curves for ATP, suramin and PPADS were constructed for each case. Protocols and times of applications were identical to the used for guinea pig P2X2 receptors.

RESULTS

Three PCR products were distinguished of 1587, 1450 and 1171 bp (Figure B.1A). The 1587 bp band corresponded to the splice variant referred as P2X2-a (Koshimizu *et al.*, 2006). The others two smallest products named P2X2-f and P2X2-g were splice variants with premature stop codons at the second exon (Figure B.2). Using nested single cell PCR we detected the presence of only mRNA of P2X2-a (Figure B.1B), therefore the others splice variants were no further characterized.

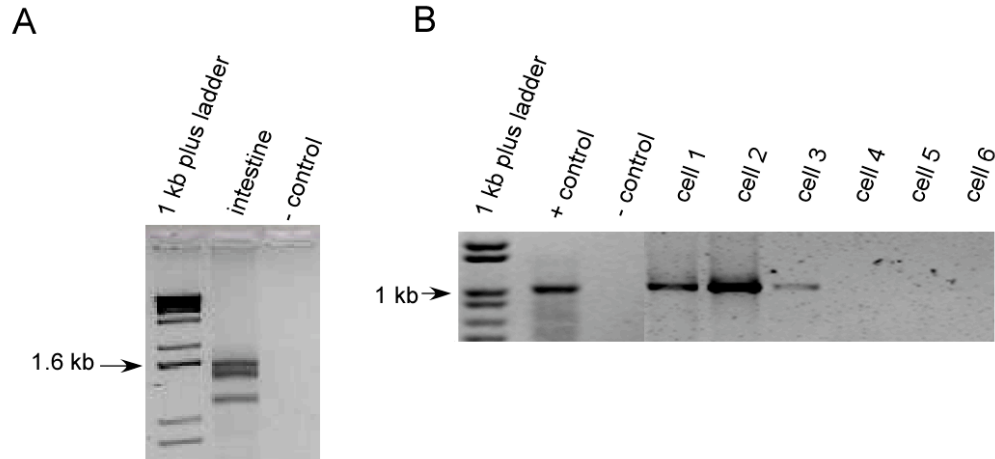


Figure B.1. Representative agarose gel electrophoresis of P2X2 RT-PCR amplification from intestine (**A**) or single neurons (**B**). Three P2X2 splice variants were isolated from intestine, negative controls were performed without template. Positive control used in B was cDNA from mouse intestine and the PCR product of 1088 bp corresponds to P2X2-a splice variant. Bands of 950 and 672 bp corresponding to P2X2-f and P2X2-g, respectively were not detected.

ATP concentration response curve was constructed using oocytes individually injected with 0.4 or 0.8 ng mRNA and we obtained an ATP-EC₅₀ value of 28±6.6 μM (Figure B.3). Two types of ATP responses were distinguished (Figure B.4A), one having an onset composed of a predominant fast component and/or other small slow component, followed by a desensitization phase (n=24). The other kind of response consisted of an onset with a fast component and a prominent slow phase, so the steady state is reached in periods longer than 4 s and desensitization is practically absent in most cases (n=6). The 80% of cells tested had kinetics similar to the first type, and 20% was like the second kind. However, some of cell showed a time dependent shift between the two types of response. We calculate a differential value of ATP-EC₅₀ of 26±5.6 μM and 63±11 μM, for cells showing the fast- and slow-onset kinetics (Figure B.4B), respectively.

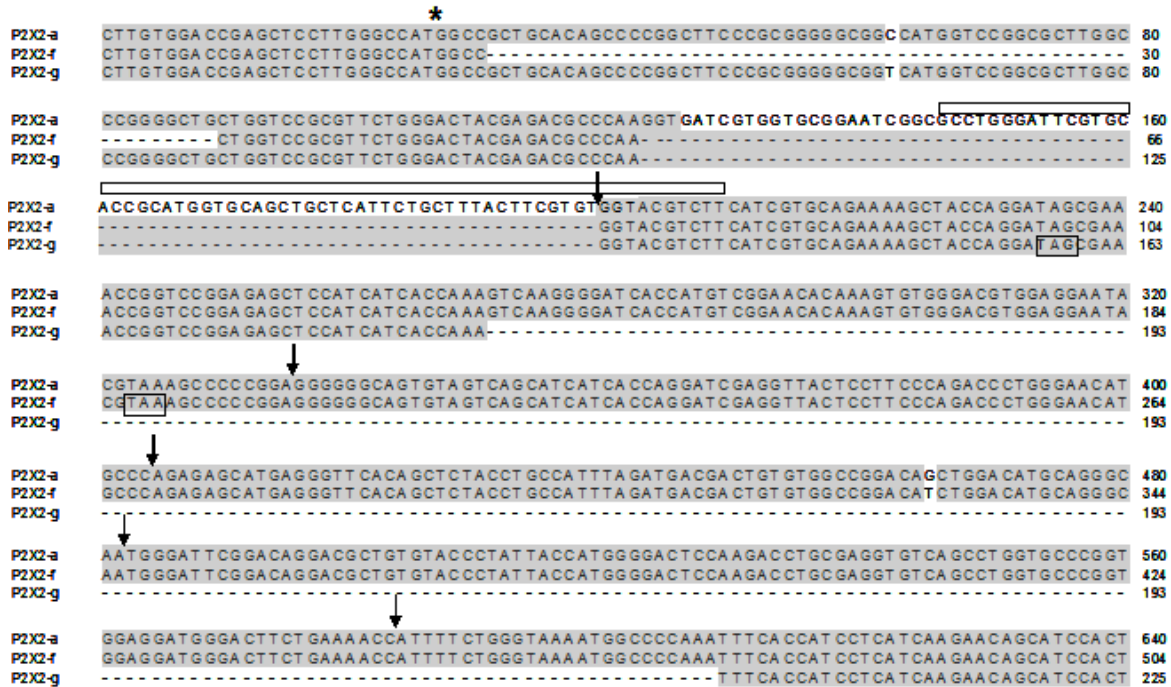


Figure B.2. ClustalV alignment of P2X2 cDNA sequences isolated from mouse intestine. Only the region where the alternative splicing occurs is shown. Start codon is indicated with an asterisk, and arrows represent the end and start of an exon, so the first arrow indicates the beginning of exon II. Nucleotides, corresponding to the transmembrane domain I, are marked with the empty bar. Alternative splicing of P2X2-f and P2X2-g change the phase and introduce premature stop codons (enclosed by a rectangle) that truncate the protein.

We tested the effects of PPADS and suramin on I_{ATP} induced by a maximal concentration of this nucleotide 1 mM. Concentration-response curves were constructed for both antagonists. PPADS inhibited the I_{ATP} in a concentration-dependent manner, with $IC_{50}=0.46\pm 0.02 \mu M$ (Figure B.5A). Complete inhibition of I_{ATP} was reached at 10 μM of PPADS. Suramin reduced the I_{ATP} with different potency in oocytes with low (-950 ± 196 nA) and high (-4360 ± 457 nA) current density (Figure B.4B), the IC_{50} s value was 0.1 ± 0.03 and $4.6\pm 1.2 \mu M$, respectively. The maximal effect of suramin was about 80% in both cases. The potency of ATP or PPADS was not modified by I_{ATP} density in the oocytes (not shown).

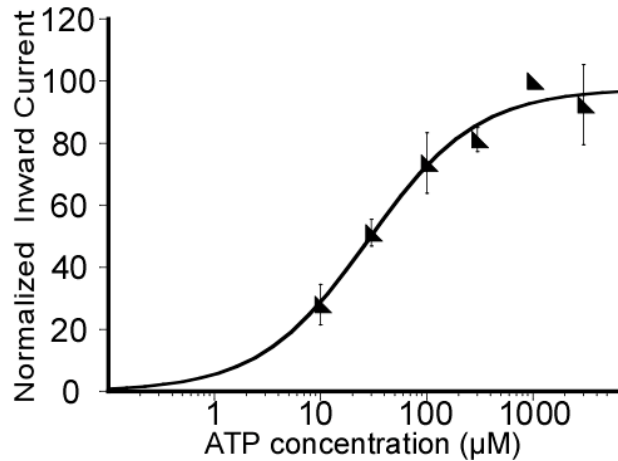


Figure B.3. Murine P2X2-a homomeric receptors are activated by ATP in a concentration-dependent manner. P2X2-a channels were expressed in *Xenopus* oocytes and ionic membrane currents were measured in response to this nucleotide. Data are well fitted with a logistic equation, yielding EC_{50} values of $28 \pm 6.6 \mu\text{M}$ (Hill coefficient 0.8 ± 0.1). Each symbol represents the average value of four to twenty experiments. Holding potential was -60 mV .

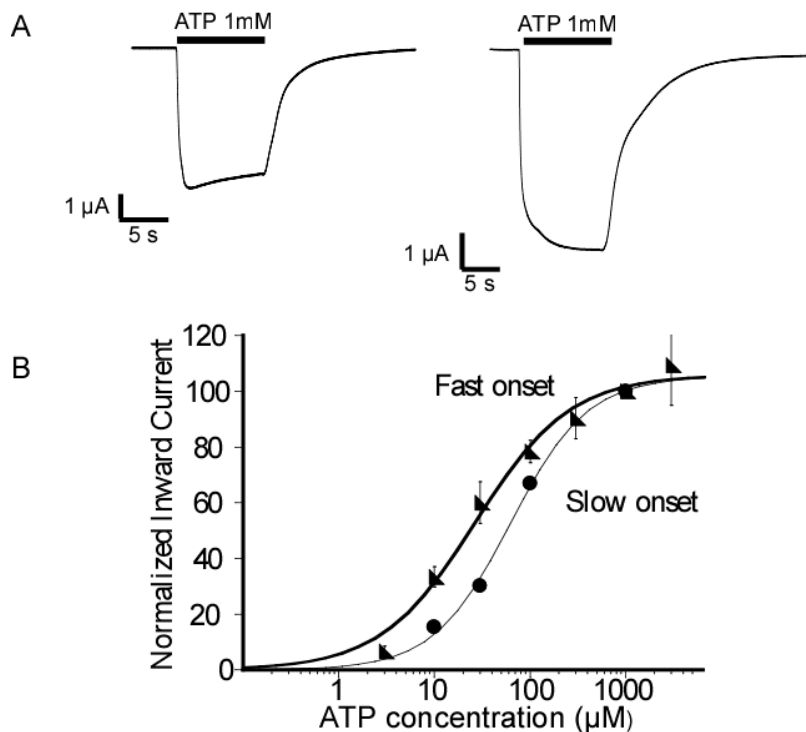


Figure B.4. Murine P2X2-a homomeric receptors display two types of kinetics. **A)** Representative traces of ATP induced-currents recorded from *Xenopus* oocytes showing two types of kinetic with fast (left) and slow (right) onsets. Holding potential was -60 mV . Horizontal bars above traces indicate the ATP application. **B)** Concentration-response curves for ATP in oocytes showing I_{ATP} with fast and slow onset showing EC_{50} s of $26 \pm 5.6 \mu\text{M}$ and $63 \pm 11 \mu\text{M}$, respectively.

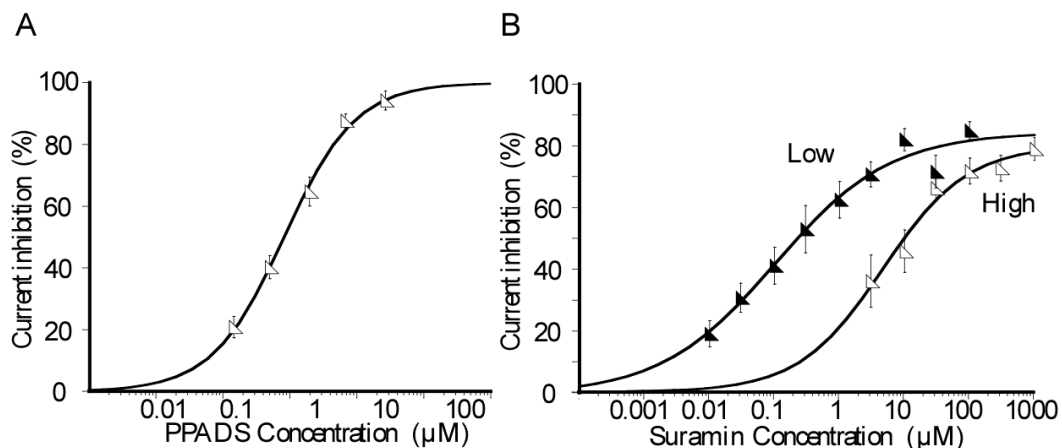


Figure B.5. PPADS and suramin inhibit P2X2-a- receptors with high potency. **A)** Concentration-response curves for the inhibitory effect of PPADS on ATP induced currents (I_{ATP}). Estimated IC_{50} was $0.46 \pm 0.02 \mu M$ ($n=4$ to 14). **B)** Concentration-response curves for the inhibitory effects of suramin on I_{ATP} mediated by P2X2-a channels in oocytes showing low (filled triangle) and high (empty triangle) current density. Estimated IC_{50} s were 0.1 ± 0.03 and $4.6 \pm 1.2 \mu M$, for low and high density, respectively. ATP 1 mM was used to activate P2X2-a receptors.

DISCUSSION

We clone three P2X2 splice variants from mouse intestine: P2X2-a, P2X2-f and P2X2-g. P2X2-a is the homologous splicing version of guinea pig P2X2-1 that retains intron 11 and was also confirmed their neuronal origin by single cell PCR. However, we do not know the cellular origin and possible role of the truncated P2X2-f and P2X2-g splice variants, because we failed to amplify them from single neurons. It is possible that these small splice variants were at very low concentration in the cells and was not detected with the strategy used. This is because we initially cloned the three variants using a super amplified cDNA (SUPER SMART) of whole intestine or culture of myenteric cells, but we cannot always amplify the smallest variants using the not super amplified cDNA. The other possibility is that P2X2-f and P2X2-g were from a non neuronal origin. In contrast to guinea pig neurons, neither the fully processed variant P2X2-2 nor P2X2-4

was detected in mouse cells, indicating a regulation species specific in the processing of P2X2 pre-mRNA.

P2X2-1 expression in *Xenopus* oocytes showed ATP potency ($EC_{50}=28 \mu\text{M}$) similar to the obtained with guinea pig P2X2-2 ($EC_{50}=22 \mu\text{M}$) receptors, and was less potent than the characterized by Koshimizu (2006) ($EC_{50}=10 \mu\text{M}$). Oocytes with two types of response differing in the onset kinetics were distinguished. We can discard that these differences were due to posttranslational modifications like glycosylations, because changes in the kinetics occurred even in the same cell after successive applications of ATP. One possible explanation is that phosphorylations or interactions with other proteins modified the I_{ATP} kinetics. A similar observation was noticed in P2X7 receptors expressed in HEK cells and it was determined to be dependent of tyrosine phosphorylation (Kim *et al.*, 2001). Density current did not modify ATP- EC_{50} or kinetics, however, cells showing slow onset were less sensitive to ATP.

Two populations of oocytes showing different suramin potency were distinguished, but this effect apparently was not seen with PPADS. We injected either 0.4 or 0.8 ng of P2X2 mRNA in oocytes, which induced current amplitudes of ~ 1 and $3.5 \mu\text{A}$, respectively. Although ATP EC_{50} s were the same (24 ± 13 and $37 \pm 7 \mu\text{M}$), suramin IC_{50} s were clearly different ($0.1 \mu\text{M}$ and $4.6 \mu\text{M}$ for low and high current density, respectively). These observations indicate that the suramin inhibitory effect is dependent of the channel density, probably through protein interactions with the long C-terminal tail. This mechanism of regulation has been suggested for P2X2 expressed in oocytes (Fujiwara *et al.*, 2004), however, the effect of suramin has not been reported to be regulated by channel density.

In P2X2 mouse receptor suramin has a monophasic effect contrary to the bifasic effect seen in guinea pig P2X2-1. Although, suramin sensitivity of mouse P2X2-a was similar to the high

sensitive phase of guinea pig P2X2-1. Probably at guinea pig P2X2 two binding sites for suramin are exposed, one with high sensitivity but low efficacy and other with low sensitivity and high efficacy. In mouse P2X2-a receptors, only the high-sensitivity binding site is evident and their efficacy is higher than in guinea pig (80% vs 18 % of inhibition). In mouse myenteric neurons suramin also inhibit in a monophasic manner ($IC_{50} = 50 \pm 18 \mu M$) (Guerrero-Alba *et al.*, 2010) similar to P2X2-a receptors, however, a comparison of their potency is difficult to assess since it seems to be affected by channel density as mentioned above.

P2X2-a channels were very sensitive to the effect of PPADS, similar than native cells ($IC_{50} = 0.6 \mu M$, (Guerrero-Alba *et al.*, 2010)). The effect of PPADS was also close to the obtained with guinea pig P2X2-1 homomeric channels (see table 2), suggesting that the mechanism of action of PPADS and binding site are more conserved than suramin between these two orthologous. PPADS potency was independently of the current amplitude and the kinetics of the ATP response.

In conclusion we found a differential expression of P2X2 splice variants between mouse and guinea pig with unique pharmacological properties. P2X2-a channels displayed characteristics, like changes in the kinetics and density dependent inhibition by suramin, that suggest that are highly regulated by different mechanism. Homomeric P2X2-a receptors may be mainly contributing to the ATP response in mouse myenteric neurons.

APPENDIX C

A. Liñan-Rico, J. Jaramillo-Polanco, R. Espinosa-Luna, J.F. Jiménez-Bremont, L. Liñan-Rico, L.M. Montaña, C. Barajas-López, **Retention of a new-defined intron changes pharmacology and kinetics of the full-length P2X2 receptor found in myenteric neurons of the guinea pig,**

Neuropharmacology, Available online 22 April 2012, ISSN 0028-3908,
10.1016/j.neuropharm.2012.04.002.
(<http://www.sciencedirect.com/science/article/pii/S0028390812001347>)

APPENDIX D

Valdez-Morales EE, Guerrero-Alba R, Liñan-Rico A, Espinosa-Luna R, Zarazua-Guzman S, Miranda-Morales M, et al. (2011). **P2X7 receptors contribute to the currents induced by ATP in guinea pig intestinal myenteric neurons.** *Eur. J. Pharmacol.* 668(3): 366-372.

REFERENCES

- Abbracchio MP, Burnstock G, Boeynaems JM, Barnard EA, Boyer JL, Kennedy C, *et al.* (2006). International Union of Pharmacology LVIII: update on the P2Y G protein-coupled nucleotide receptors: from molecular mechanisms and pathophysiology to therapy. *Pharmacol Rev* **58**(3): 281-341.
- Agboh KC, Webb TE, Evans RJ, Ennion SJ (2004). Functional characterization of a P2X receptor from *Schistosoma mansoni*. *J Biol Chem* **279**(40): 41650-41657.
- Antonio LS, Stewart AP, Xu XJ, Varanda WA, Murrell-Lagnado RD, Edwardson JM (2011). P2X4 receptors interact with both P2X2 and P2X7 receptors in the form of homotrimers. *Br J Pharmacol* **163**(5): 1069-1077.
- Barajas-Lopez C, Barrientos M, Espinosa-Luna R (1993a). Suramin increases the efficacy of ATP to activate an inward current in myenteric neurons from guinea-pig ileum. *Eur J Pharmacol* **250**(1): 141-145.
- Barajas-Lopez C, Espinosa-Luna R, Christofi FL (2000). Changes in intracellular Ca²⁺ by activation of P2 receptors in submucosal neurons in short-term cultures. *Eur J Pharmacol* **409**(3): 243-257.
- Barajas-Lopez C, Huizinga JD (1993b). New transmitters and new targets in the autonomic nervous system. *Curr Opin Neurobiol* **3**(6): 1020-1027.
- Barajas-Lopez C, Huizinga JD, Collins SM, Gerzanich V, Espinosa-Luna R, Peres AL (1996a). P2x-purinoceptors of myenteric neurones from the guinea-pig ileum and their unusual pharmacological properties. *Br J Pharmacol* **119**(8): 1541-1548.
- Barajas-Lopez C, Montano LM, Espinosa-Luna R (2002). Inhibitory interactions between 5-HT₃ and P2X channels in submucosal neurons. *Am J Physiol Gastrointest Liver Physiol* **283**(6): G1238-1248.
- Barajas-Lopez C, Peres AL, Espinosa-Luna R (1996b). Cellular mechanisms underlying adenosine actions on cholinergic transmission in enteric neurons. *Am J Physiol* **271**(1 Pt 1): C264-275.
- Barajas L, Liu L (1993). The renal nerves in the newborn rat. *Pediatr Nephrol* **7**(5): 657-666.
- Bavan S, Straub VA, Blaxter ML, Ennion SJ (2009). A P2X receptor from the tardigrade species *Hypsibius dujardini* with fast kinetics and sensitivity to zinc and copper. *BMC Evol Biol* **9**: 17.
- Blencowe BJ (2006). Alternative splicing: new insights from global analyses. *Cell* **126**(1): 37-47.
- Blom N, Gammeltoft S, Brunak S (1999). Sequence and structure-based prediction of eukaryotic protein phosphorylation sites. *Journal of molecular biology* **294**(5): 1351-1362.

- Boue-Grabot E, Archambault V, Seguela P (2000). A Protein Kinase C Site Highly Conserved in P2X Subunits Controls the Desensitization Kinetics of P2X2 ATP-gated Channels 10.1074/jbc.275.14.10190. *J. Biol. Chem.* **275**(14): 10190-10195.
- Brake AJ, Wagenbach MJ, Julius D (1994). New structural motif for ligand-gated ion channels defined by an ionotropic ATP receptor. *Nature* **371**(6497): 519-523.
- Brandle U, Spielmanns P, Osteroth R, Sim J, Surprenant A, Buell G, *et al.* (1997). Desensitization of the P2X(2) receptor controlled by alternative splicing. *FEBS Lett* **404**(2-3): 294-298.
- Brookes SJ (2001). Classes of enteric nerve cells in the guinea-pig small intestine. *Anat Rec* **262**(1): 58-70.
- Buell G, Lewis C, Collo G, North RA, Surprenant A (1996). An antagonist-insensitive P2X receptor expressed in epithelia and brain. *Embo J* **15**(1): 55-62.
- Burge C, Karlin S (1997). Prediction of complete gene structures in human genomic DNA. *Journal of molecular biology* **268**(1): 78-94.
- Burnstock G (2006). Historical review: ATP as a neurotransmitter. *Trends Pharmacol Sci* **27**(3): 166-176.
- Burnstock G (2007). Purine and pyrimidine receptors. *Cell Mol Life Sci* **64**(12): 1471-1483.
- Burnstock G (2009). Purinergic cotransmission. *Exp Physiol* **94**(1): 20-24.
- Burnstock G (2002). Purinergic signaling and vascular cell proliferation and death. *Arterioscler Thromb Vasc Biol* **22**(3): 364-373.
- Burnstock G, Knight GE (2004). Cellular distribution and functions of P2 receptor subtypes in different systems. *Int Rev Cytol* **240**: 31-304.
- Burnstock G, Verkhratsky A (2009). Evolutionary origins of the purinergic signalling system. *Acta Physiol (Oxf)* **195**(4): 415-447.
- Castelucci P, Robbins HL, Poole DP, Furness JB (2002). The distribution of purine P2X(2) receptors in the guinea-pig enteric nervous system. *Histochem Cell Biol* **117**(5): 415-422.
- Chen C, Parker MS, Barnes AP, Deininger P, Bobbin RP (2000). Functional Expression of Three P2X2 Receptor Splice Variants From Guinea Pig Cochlea. *J Neurophysiol* **83**(3): 1502-1509.
- Clyne JD, Brown TC, Hume RI (2003). Expression level dependent changes in the properties of P2X2 receptors. *Neuropharmacology* **44**(3): 403-412.
- Coddou C, Yan Z, Obsil T, Huidobro-Toro JP, Stojilkovic SS (2011). Activation and regulation of purinergic P2X receptor channels. *Pharmacol Rev* **63**(3): 641-683.

- Eickhorst AN, Berson A, Cockayne D, Lester HA, Khakh BS (2002). Control of P2X(2) channel permeability by the cytosolic domain. *J Gen Physiol* **120**(2): 119-131.
- Evans RJ, Lewis C, Buell G, Valera S, North RA, Surprenant A (1995). Pharmacological characterization of heterologously expressed ATP-gated cation channels (P2x purinoceptors). *Mol Pharmacol* **48**(2): 178-183.
- Fackenthal JD, Godley LA (2008). Aberrant RNA splicing and its functional consequences in cancer cells. *Dis Model Mech* **1**(1): 37-42.
- Feng YH, Li X, Wang L, Zhou L, Gorodeski GI (2006). A truncated P2X7 receptor variant (P2X7-j) endogenously expressed in cervical cancer cells antagonizes the full-length P2X7 receptor through hetero-oligomerization. *J Biol Chem* **281**(25): 17228-17237.
- Fountain SJ, Burnstock G (2009). An evolutionary history of P2X receptors. *Purinergic Signal* **5**(3): 269-272.
- Fujiwara Y, Kubo Y (2004). Density-dependent changes of the pore properties of the P2X2 receptor channel. *J Physiol* **558**(Pt 1): 31-43.
- Fujiwara Y, Kubo Y (2006). Regulation of the desensitization and ion selectivity of ATP-gated P2X2 channels by phosphoinositides. *J Physiol* **576**(Pt 1): 135-149.
- Furness JB, Costa M (1980). Types of nerves in the enteric nervous system. *Neuroscience* **5**(1): 1-20.
- Galligan JJ (2002). Ligand-gated ion channels in the enteric nervous system. *Neurogastroenterol Motil* **14**(6): 611-623.
- Galligan JJ, Bertrand PP (1994). ATP mediates fast synaptic potentials in enteric neurons. *J Neurosci* **14**(12): 7563-7571.
- Gever JR, Cockayne DA, Dillon MP, Burnstock G, Ford AP (2006). Pharmacology of P2X channels. *Pflugers Arch* **452**(5): 513-537.
- Glushakow AV, Glushakova HY, Skok VI (1998). Two types of P2X-purinoceptors in neurons of the guinea pig ileum submucous plexus. *Neurophysiology* **30**, **30**: 301-304.
- Guerrero-Alba R, Valdez-Morales E, Juarez EH, Miranda-Morales M, Ramirez-Martinez JF, Espinosa-Luna R, *et al.* (2010). Two suramin binding sites are present in guinea pig but only one in murine native P2X myenteric receptors. *Eur J Pharmacol* **626**(2-3): 179-185.
- Guimaraes MZ (2008). Isoform specificity of P2X2 purinergic receptor C-terminus binding to tubulin. *Neurochem Int* **52**(1-2): 314-320.

- Hebsgaard SM, Korning PG, Tolstrup N, Engelbrecht J, Rouze P, Brunak S (1996). Splice site prediction in *Arabidopsis thaliana* pre-mRNA by combining local and global sequence information. *Nucleic Acids Res* **24**(17): 3439-3452.
- Hu HZ, Gao N, Lin Z, Gao C, Liu S, Ren J, *et al.* (2001). P2X(7) receptors in the enteric nervous system of guinea-pig small intestine. *J Comp Neurol* **440**(3): 299-310.
- Jones DT, Taylor WR, Thornton JM (1994). A model recognition approach to the prediction of all-helical membrane protein structure and topology. *Biochemistry* **33**(10): 3038-3049.
- Kawate T, Michel JC, Birdsong WT, Gouaux E (2009). Crystal structure of the ATP-gated P2X(4) ion channel in the closed state. *Nature* **460**(7255): 592-598.
- Kenakin R (1993). Pharmacologic Analysis of Drug-receptor Interaction. *2nd Ed. Raven Press, Ltd., New York, N.Y.*
- Khakh BS (2001). Molecular physiology of P2X receptors and ATP signalling at synapses. *Nat Rev Neurosci* **2**(3): 165-174.
- Khakh BS, North RA (2006). P2X receptors as cell-surface ATP sensors in health and disease. *Nature* **442**(7102): 527-532.
- Kim E, Goren A, Ast G (2008). Alternative splicing: current perspectives. *Bioessays* **30**(1): 38-47.
- Kim M, Jiang LH, Wilson HL, North RA, Surprenant A (2001). Proteomic and functional evidence for a P2X7 receptor signalling complex. *Embo J* **20**(22): 6347-6358.
- King BF, Townsend-Nicholson A, Wildman SS, Thomas T, Spyer KM, Burnstock G (2000). Coexpression of rat P2X2 and P2X6 subunits in *Xenopus* oocytes. *J Neurosci* **20**(13): 4871-4877.
- Koshimizu T-a, Kretschmannova K, He M-L, Ueno S, Tanoue A, Yanagihara N, *et al.* (2006). Carboxyl-Terminal Splicing Enhances Physical Interactions between the Cytoplasmic Tails of Purinergic P2X Receptors. *Mol Pharmacol* **69**(5): 1588-1598.
- Koshimizu T-a, Tomic M, Van Goor F, Stojilkovic SS (1998). Functional Role of Alternative Splicing in Pituitary P2X2 Receptor-Channel Activation and Desensitization 10.1210/me.12.7.901. *Mol Endocrinol* **12**(7): 901-913.
- Koshimizu T, Koshimizu M, Stojilkovic SS (1999). Contributions of the C-terminal domain to the control of P2X receptor desensitization. *J Biol Chem* **274**(53): 37651-37657.
- Kucenas S, Li Z, Cox JA, Egan TM, Voigt MM (2003). Molecular characterization of the zebrafish P2X receptor subunit gene family. *Neuroscience* **121**(4): 935-945.
- Kunze WA, Furness JB (1999). The enteric nervous system and regulation of intestinal motility. *Annu Rev Physiol* **61**: 117-142.

- Le KT, Babinski K, Seguela P (1998). Central P2X4 and P2X6 channel subunits coassemble into a novel heteromeric ATP receptor. *J Neurosci* **18**(18): 7152-7159.
- Le KT, Boue-Grabot E, Archambault V, Seguela P (1999). Functional and biochemical evidence for heteromeric ATP-gated channels composed of P2X1 and P2X5 subunits. *J Biol Chem* **274**(22): 15415-15419.
- Li Z, Migita K, Samways DS, Voigt MM, Egan TM (2004). Gain and loss of channel function by alanine substitutions in the transmembrane segments of the rat ATP-gated P2X2 receptor. *J Neurosci* **24**(33): 7378-7386.
- Liu L, Barajas L (1993). The rat renal nerves during development. *Anat Embryol (Berl)* **188**(4): 345-361.
- Lynch KJ, Touma E, Niforatos W, Kage KL, Burgard EC, van Biesen T, *et al.* (1999). Molecular and Functional Characterization of Human P2X2 Receptors. *Mol Pharmacol* **56**(6): 1171-1181.
- Masin M, Kerschensteiner D, Dumke K, Rubio ME, Soto F (2006). Fe65 Interacts with P2X2 Subunits at Excitatory Synapses and Modulates Receptor Function. *J. Biol. Chem.* **281**(7): 4100-4108.
- Murrell-Lagnado RD, Qureshi OS (2008). Assembly and trafficking of P2X purinergic receptors (Review). *Mol Membr Biol* **25**(4): 321-331.
- Nicke A, Kerschensteiner D, Soto F (2005). Biochemical and functional evidence for heteromeric assembly of P2X1 and P2X4 subunits. *J Neurochem* **92**(4): 925-933.
- Nilsen TW, Graveley BR (2010). Expansion of the eukaryotic proteome by alternative splicing. *Nature* **463**(7280): 457-463.
- North RA (2002). Molecular physiology of P2X receptors. *Physiol Rev* **82**(4): 1013-1067.
- North RA, Barnard EA (1997). Nucleotide receptors. *Curr Opin Neurobiol* **7**(3): 346-357.
- North RA, Surprenant A (2000). Pharmacology of Cloned P2X Receptors
doi:10.1146/annurev.pharmtox.40.1.563. *Annual Review of Pharmacology and Toxicology* **40**(1): 563-580.
- Pan YX, Xu J, Bolan E, Moskowitz HS, Xu M, Pasternak GW (2005). Identification of four novel exon 5 splice variants of the mouse mu-opioid receptor gene: functional consequences of C-terminal splicing. *Mol Pharmacol* **68**(3): 866-875.
- Pankratov Y, Lalo U, Verkhratsky A, North RA (2006). Vesicular release of ATP at central synapses. *Pflugers Arch* **452**(5): 589-597.
- Parker MS, Larroque ML, Campbell JM, Bobbin RP, Deininger PL (1998). Novel variant of the P2X2 ATP receptor from the guinea pig organ of Corti. *Hear Res* **121**(1-2): 62-70.

- Pelegrin P, Surprenant A (2009). The P2X(7) receptor-pannexin connection to dye uptake and IL-1beta release. *Purinergic Signal* **5**(2): 129-137.
- Poole DP, Castelucci P, Robbins HL, Chiochetti R, Furness JB (2002). The distribution of P2X3 purine receptor subunits in the guinea pig enteric nervous system. *Auton Neurosci* **101**(1-2): 39-47.
- Radford KM, Virginio C, Surprenant A, North RA, Kawashima E (1997). Baculovirus expression provides direct evidence for heteromeric assembly of P2X2 and P2X3 receptors. *J Neurosci* **17**(17): 6529-6533.
- Ralevic V, Burnstock G (1998). Receptors for purines and pyrimidines. *Pharmacol Rev* **50**(3): 413-492.
- Ren J, Bian X, DeVries M, Schnegelsberg B, Cockayne DA, Ford APDW, *et al.* (2003). P2X2 subunits contribute to fast synaptic excitation in myenteric neurons of the mouse small intestine. *J Physiol (Lond)* **552**(3): 809-821.
- Roberts JA, Vial C, Digby HR, Agboh KC, Wen H, Atterbury-Thomas A, *et al.* (2006). Molecular properties of P2X receptors. *Pflugers Arch* **452**(5): 486-500.
- Ruan HZ, Burnstock G (2005). The distribution of P2X 5 purinergic receptors in the enteric nervous system of mouse. *Cell and Tissue Research* **319**(2): 191-200.
- Salih SG, Housley GD, Burton LD, Greenwood D (1998). P2X2 receptor subunit expression in a subpopulation of cochlear type I spiral ganglion neurones. *Neuroreport* **9**(2): 279-282.
- Sim JA, Broomhead HE, North RA (2008). Ectodomain lysines and suramin block of P2X1 receptors. *J Biol Chem* **283**(44): 29841-29846.
- Simon J, Kidd EJ, Smith FM, Chessell IP, Murrell-Lagnado R, Humphrey PPA, *et al.* (1997). Localization and Functional Expression of Splice Variants of the P2X2 Receptor. *Mol Pharmacol* **52**(2): 237-248.
- Surprenant A, Buell G, North RA (1995). P2X receptors bring new structure to ligand-gated ion channels. *Trends Neurosci* **18**(5): 224-229.
- Tittle RK, Hume RI (2008). Opposite effects of zinc on human and rat P2X2 receptors. *J Neurosci* **28**(44): 11131-11140.
- Torres GE, Egan TM, Voigt MM (1999). Hetero-oligomeric assembly of P2X receptor subunits. Specificities exist with regard to possible partners. *J Biol Chem* **274**(10): 6653-6659.
- Trams EG (1981). On the evolution of neurochemical transmission. *Differentiation* **19**(3): 125-133.

Troyanovskaya M, Wackym PA (1998). Evidence for three additional P2X2 purinoceptor isoforms produced by alternative splicing in the adult rat vestibular end-organs. *Hear Res* **126**(1-2): 201-209.

Valdez-Morales EE, Guerrero-Alba R, Liñan-Rico A, Espinosa-Luna R, Zarazua-Guzman S, Miranda-Morales M, *et al.* (2011). P2X7 receptors contribute to the currents induced by ATP in guinea pig intestinal myenteric neurons. *Eur. J. Pharmacol.* **668**(3): 366-372.

Valera S, Hussy N, Evans RJ, Adami N, North RA, Surprenant A, *et al.* (1994). A new class of ligand-gated ion channel defined by P2x receptor for extracellular ATP. *Nature* **371**(6497): 516-519.

Virginio C, MacKenzie A, Rassendren FA, North RA, Surprenant A (1999). Pore dilation of neuronal P2X receptor channels. *Nat Neurosci* **2**(4): 315-321.

Webb TE, Simon J, Krishek BJ, Bateson AN, Smart TG, King BF, Burnstock G, Barnard EA, (1993). Cloning and functional expression of a brain G-protein-coupled ATP receptor. *FEBS Lett* **324**(2): 219-225.

Zemkova H, He ML, Koshimizu TA, Stojilkovic SS (2004). Identification of ectodomain regions contributing to gating, deactivation, and resensitization of purinergic P2X receptors. *J Neurosci* **24**(31): 6968-6978.

SUPPLEMENTARY MATERIAL

A

		Exon I	
genP2x2	CCCCTC--CGAGCTCCAGCCTCCCTCCTCCGGCACCTGCGGCACGCAGTGGGGCCCTGGGTGGTGCAGCCCGAGAGCAG		78
AF053327.1	CCACGCTCCGGCTCCAGCCTCCCTCCTCCGGCACCTGCGGCACCGGATGGGGCCCTGGGTGGTGCAGCCCGAGAGCAG		80
P2X2-1	-----		0
genP2x2f3	-----		0
genP2x2	GGTTCGGGCACCATGGCTGCCACCCACCCCAAGGCCCCACAGCGCAGCGCCTGGCCCAAGGCTGCTGGTCTGCATTCT		158
AF053327.1	GGTTCGGGCACCATGGCTGCCACCCACCCCAAGGCCCCACAGCGCAGCGCCTGGCCCAAGGCTGCTGGTCTGCATTCT		157
P2X2-1	-GTTCTGGGCACCATGGCTGCCACCCACCCCAAGGCCCCACAGCGCAGCGCCTGGCCCAAGGCTGCTGGTCTGCATTCT		79
genP2x2f3	-----		0
genP2x2	GGGACTACGAGACGCCCAAGGTGATCGTGGTGCACAACCGCGCCTGGGGTCTGTACCGGGCGGTGCAGCTGCTCATC		238
AF053327.1	GGGACTACGAGACGCCCAAGGTGATCGTGGTGCACAACCGCGCCTGGGGTCTGTACCGGGCGGTGCAGCTGCTCATC		237
P2X2-1	GGGACTACGAGACGCCCAAGGTGATCGTGGTGCACAACCGCGCCTGGGGTCTGTACCGGGCGGTGCAGCTGCTCATC		159
genP2x2f3	-----		0
Intron 1			
genP2x2	CTGCTCTACTTTGTGTGGTGCAGGGCGTGGCGGGTGGGGATGGGGACCGGATCCTGGGTGCCGGGTGGAGTCAGG		318
AF053327.1	CTGCTCTACTTTGTGTGGT-----		256
P2X2-1	CTGCTCTACTTTGTGTGGT-----		178
genP2x2f3	-----		0
genP2x2	GCAGGGACTGGGGACCTGTGCTGGGAGCACAGGGGAGCCTGGGCACAGGGCTGGAGTCAGGGCGGGAGCTGGGAGAAGG		398
AF053327.1	-----		256
P2X2-1	-----		178
genP2x2f3	-----		0
genP2x2	GAGCCTGGGTGCAGGGCTTGGGGCAGAGACGGGGCCCTGGGTGCTGGGGTGGATACCAACTGGGAAGGGTGAGCTCAG		478
AF053327.1	-----		256
P2X2-1	-----		178
genP2x2f3	-----		0
genP2x2	CTGAGGGGGCTCTGGCTCCCATGCAGGGGTAGGGCTGGCAGTAAGCAGCACAGGGCTGGGAAGGAGCCAAGCAGAGG		558
AF053327.1	-----		256
P2X2-1	-----		178
genP2x2f3	-----		0
Exon II			
genP2x2	AAGTGGGGAGCTGGGCTGGGTGGGGACAACATCGCACAGGAGGCTGGGGCCCTGCAGGTACGTGTTTCATCGTCAGAAGA		638
AF053327.1	-----ACGTGTTTCATCGTCAGAAGA		277
P2X2-1	-----ACGTGTTTCATCGTCAGAAGA		199
genP2x2f3	-----		0
genP2x2	GCTACCAGGACAGCGAGACGGGCCCCGAGAGCTCCATCATTACCAAGGTCAAGGGGATCACACAGTCTGAGCACAAAGTG		718
AF053327.1	GCTACCAGGACAGCGAGACGGGCCCCGAGAGCTCCATCATTACCAAGGTCAAGGGGATCACACAGTCTGAGCACAAAGTG		357
P2X2-1	GCTACCAGGACAGCGAGACGGGCCCCGAGAGCTCCATCATTACCAAGGTCAAGGGGATCACACAGTCTGAGCACAAAGTG		279
genP2x2f3	-----		0
Intron 2			
genP2x2	TGGGACGTGGAGGAGTATGTGAAGCCCCCTGAGGTGCGGCCCTCCCGAGCCCTGTCCTGCCTCAGGCCCAAGCTGAGA		798
AF053327.1	TGGGACGTGGAGGAGTATGTGAAGCCCCCTGAGG-----		391
P2X2-1	TGGGACGTGGAGGAGTATGTGAAGCCCCCTGAGG-----		313
genP2x2f3	-----		0
Exon III			
genP2x2	GCTGGCTGGCCACTGCTCCCTCTCTCCATCCAGGGGGCAGTGTGTTTCAGCATCATCACCAGGATTGAGGTCACCCCT		878
AF053327.1	-----GGGGCAGTGTGTTTCAGCATCATCACCAGGATTGAGGTCACCCCT		436
P2X2-1	-----GGGGCAGTGTGTTTCAGCATCATCACCAGGATTGAGGTCACCCCT		358
genP2x2f3	-----		0
Intron 3			
genP2x2	TCCAGACCCTGGGTGCCTGCCAGAGGTGAGGGCAGTGGAGGGAGCCAGGGAGCAGCCCTGGCAATCTGCAGGGTGGCTC		958
AF053327.1	TCCAGACCCTGGGTGCCTGCCAGAG-----		462
P2X2-1	TCCAGACCCTGGGTGCCTGCCAGAG-----		384
genP2x2f3	-----		0
Exon IV			
genP2x2	TCTGATTCCCTCTGCACCCCTAGAGCATAAGGGTCCCCAACACCACCTGCCACTTGGATGCTGACTGCACAGCTGGAGAGC		1038
AF053327.1	-----AGCATAAGGGTCCCCAACACCACCTGCCACTTGGATGCTGACTGCACAGCTGGAGAGC		520
P2X2-1	-----AGCATAAGGGTCCCCAACACCACCTGCCACTTGGATGCTGACTGCACAGCTGGAGAGC		442
genP2x2f3	-----		0
Intron 4			
genP2x2	TGGACATGCTGGGCAATGGTTCAGTGGTTCGCCGGGTGGCTGGGTGGGCTGCAGCTGGGCAGAAATGAACCAGTGTGTGC		1118
AF053327.1	TGGACATGCTGGGCAATGG-----		539
P2X2-1	TGGACATGCTGGGCAATGG-----		461
genP2x2f3	-----		0
Exon V			
genP2x2	CCTGCAGGGCTGCGGACAGGGCGCTGCGTGCCCTACTACCATGGGGAGGCCAAGACCTGCGAGGTGTCGGGTGGTGTCC		1198
AF053327.1	-----GCTGCGGACAGGGCGCTGCGTGCCCTACTACCATGGGGAGGCCAAGACCTGCGAGGTGTCGGGTGGTGTCC		611
P2X2-1	-----GCTGCGGACAGGGCGCTGCGTGCCCTACTACCATGGGGAGGCCAAGACCTGCGAGGTGTCGGGTGGTGTCC		533
genP2x2f3	-----		0

 Intron 5		
genP2x2	AGTGGAGGATGGGGCCGAGTCAGGTGCGCAGTCCCTCCATGGGCAGAGGGCAGCAATGGGGCAGGAAGGGGTCCCT	1278
AF053327.1	AGTGGAGGATGGGGCCGAGTCAG-----	635
P2X2-1	AGTGGAGGATGGGGCCGAGTCAG-----	557
genP2x2f3	-----	0
 Exon VI		
genP2x2	CACATCCCTGTCTGTTCCTCCAGCCACTTCTGGGTAAGATGGCCCCAAACTTCACCATCCTCATCAAGAACAGCATCCA	1358
AF053327.1	-----CCACTTCTGGGTAAGATGGCCCCAAACTTCACCATCCTCATCAAGAACAGCATCCA	692
P2X2-1	-----CCACTTCTGGGTAAGATGGCCCCAAACTTCACCATCCTCATCAAGAACAGCATCCA	614
genP2x2f3	-----	0
 Intron 6		
genP2x2	CTACCCCAAGTTCAGTTCCTCAAGTAAGAGTCAGCAGGGCTGGGGCTGGCACGGGCATCTGGGACAGGGTGTGGGGTT	1438
AF053327.1	CTACCCCAAGTTCAGTTCCTCAAG-----	717
P2X2-1	CTACCCCAAGTTCAGTTCCTCAAG-----	639
genP2x2f3	-----	0
 Exon VII		
genP2x2	CCAGGCCTCTGCCACTCCTAGGGCAACATTGCACACCGGGAGGATGACT-ACCTGAGGCGCTGCACCTTCGATCAGGGC	1517
AF053327.1	-----GGCAACATTGCACACCGGGAGGATGACT-ACCTGAGGCGCTGCACCTTCGATCAGGGC	774
P2X2-1	-----GGCAACATTGCACACCGGGAGGATGACT-ACCTGAGGCGCTGCACCTTCGATCAGGGC	696
genP2x2f3	-----	0
genP2x2	TTTGACCCTACTGCCCATCTTCCGGCTGGGCTTCATTGTGGAGCAGGCTGGGGAGAACTTCACAGAGCTGGCACACAG	1597
AF053327.1	TTTGACCCTACTGCCCATCTTCCGGCTGGGCTTCATTGTGGAGCAGGCTGGGGAGAACTTCACAGAGCTGGCACACAG	854
P2X2-1	TTTGACCCTACTGCCCATCTTCCGGCTGGGCTTCATTGTGGAGCAGGCTGGGGAGAACTTCACAGAGCTGGCACACAG	776
genP2x2f3	-----TTACAGAGCTGGCACACAG	20
 Intron 7		
genP2x2	GGTGAGAAGGGCTCCTCCTCTCAGAGAGCCACGCTACAGGACACAACACTCCCCAGCACATGCTCCTGGGCTGACCCCT	1677
AF053327.1	GG-----	856
P2X2-1	GG-----	778
genP2x2f3	GGTGAGAAGGGCTCCTCCTCTCAGAGAGCCACGCTACAGGACACAACACTCCCCAGCACATGCTCCTGGGCTGACCCCT	100
 Exon VIII		
genP2x2	CCTCCTGCCCTTCCCTTG CAGGGTGGTGTATTGGCGTCATCATCAACTGGGACTGTGACCTGGACCTGCCTCATCCCAC	1757
AF053327.1	-----GTGGTGTATTGGCGTCATCATCAACTGGGACTGTGACCTGGACCTGCCTCATCCCAC	915
P2X2-1	-----GTGGTGTATTGGCGTCATCATCAACTGGGACTGTGACCTGGACCTGCCTCATCCCAC	837
genP2x2f3	CCTCCTGCCCTTCCCTTG CAGGGTGGTGTATTGGCGTCATCATCAACTGGGACTGTGACCTGGACCTGCCTCATCCCAC	180
 Intron 8		
genP2x2	TGCAACCTAAATACTCCTTTCGGAGGCTCGACCCCAACACGCTCCCCGCTCCTCAGGCTACAACCTTCAGGTACCTTCC	1837
AF053327.1	TGCAACCTAAATACTCCTTTCGGAGGCTCGACCCCAACACGCTCCCCGCTCCTCAGGCTACAACCTTCAGGT-----	988
P2X2-1	TGCAACCTAAATACTCCTTTCGGAGGCTCGACCCCAACACGCTCCCCGCTCCTCAGGCTACAACCTTCAGGT-----	910
genP2x2f3	TGCAACCTAAATACTCCTTTCGGAGGCTCGACCCCAACACGCTCCCCGCTCCTCAGGCTACAACCTTCAGGTACCTTCC	260
 Exon IX		
genP2x2	CAGAGTGCCCTGGAGAGGAAAAATGGCCAGTGGGCATGCATTTCTGCTGGGCAGGGCTCGCTTACCCAGGTTTGCCA	1917
AF053327.1	-----TTGCCA	994
P2X2-1	-----TTGCCA	916
genP2x2f3	CAGAGTGCCCTGGAGAGGAAAAATGGCCAGTGGGCATGCATTTCTGCTGGGCAGGGCTCGCTTACCCAGGTTTGCCA	340
genP2x2	AGTACTACCGAGTGAACAGCACCACCACCCGCACACTCATCAAGGCATATGGGATTTCGCATCGATGTCATCGTGACCGGT	1997
AF053327.1	AGTACTACCGAGTGAACAGCACCACCACCACCCGCACACTCATCAAGGCATATGGGATTTCGCATCGATGTCATCGTGACCGGT	1074
P2X2-1	AGTACTACCGAGTGAACAGCACCACCACCACCCGCACACTCATCAAGGCATATGGGATTTCGCATCGATGTCATCGTGACCGGT	996
genP2x2f3	AGTACTACCGAGTGAACAGCACCACCACCACCCGCACACTCATCAAGGCATATGGGATTTCGCATCGATGTCATCGTGACCGGT	420
 Intron 9		
genP2x2	CAGGTAATGTGGTGCCAAAGCCACCTGCTCAGTCCCTGCAGGCCCTGGCAGCCCTACAGGCTGACCAAGCCCATCCCA	2077
AF053327.1	CAGG-----	1078
P2X2-1	CAGG-----	1000
genP2x2f3	CAGGTAATGTGGTGCCAAAGCCACCTGCTCAGTCCCTGCAGGCCCTGGCAGCCCTACAGGCTGACCAAGCCCATCCCA	500
 Exon X		
genP2x2	CCCAGGCAGGGAAGTTTCAGCCTGATTTCCACCATCATCAACCTGGCCACTGCGCTGACCTCCATTGGAGTGGTAAGGAAT	2157
AF053327.1	-----CAGGGAAGTTTCAGCCTGATTTCCACCATCATCAACCTGGCCACTGCGCTGACCTCCATTGGAGTGG-----	1144
P2X2-1	-----CAGGGAAGTTTCAGCCTGATTTCCACCATCATCAACCTGGCCACTGCGCTGACCTCCATTGGAGTGG-----	1066
genP2x2f3	CCCAGGCAGGGAAGTTTCAGCCTGATTTCCACCATCATCAACCTGGCCACTGCGCTGACCTCCATTGGAGTGGTAAGGAAT	580
 Exon XI		
genP2x2	CCACTTGGGGACTGGGTGGGGTTGGGGGGGGTTGCAGGCTCCTTACCCTGGTCTCTACCTGCCTTAGGGCTCCTTCC	2237
AF053327.1	-----GCTCCTTCC	1153
P2X2-1	-----GCTCCTTCC	1075
genP2x2f3	CCACTTGGGGACTGGGTGGGGTTGGGGGGGGTTGCAGGCTCCTTACCCTGGTCTCTACCTGCCTTAGGGCTCCTTCC	660
 Intron 11		
genP2x2	TGTGTGACTGGATCTTGCTAACATTTCATGAACAAAAACAAGGCTACAGCCATAAGAAAATTTGACAAGGTGTGTGCGCCA	2317
AF053327.1	TGTGTGACTGGATCTTGCTAACATTTCATGAACAAAAACAAGGCTACAGCCATAAGAAAATTTGACAAGGTGTGTGCGCCA	1233
P2X2-1	TGTGTGACTGGATCTTGCTAACATTTCATGAACAAAAACAAGGCTACAGCCATAAGAAAATTTGACAAGGTGTGTGCGCCA	1155
genP2x2f3	TGTGTGACTGGATCTTGCTAACATTTCATGAACAAAAACAAGGCTACAGCCATAAGAAAATTTGACAAGGTGTGTGCGCCA	740
genP2x2	AGCCGGCCCTCCAGCAGCTGGCCAGTGCACCTTGCTCTTATTCTGGGCCAGGCTCCCCACCACCCAGGCAGTCTCTCA	2397
AF053327.1	AGCCGGCCCTCCAGCAGCTGGCCAGTGCACCTTGCTCTTATTCTGGGCCAGGCTCCCCACCACCCAGGCAGTCTCTCA	1312
P2X2-1	AGCCGGCCCTCCAGCAGCTGGCCAGTGCACCTTGCTCTTATTCTGGGCCAGGCTCCCCACCACCCAGGCAGTCTCTCA	1235
genP2x2f3	AGCCGGCCCTCCAGCAGCTGGCCAGTGCACCTTGCTCTTATTCTGGGCCAGGCTCCCCACCACCCAGGCAGTCTCTCA	820
genP2x2	GTCCTTGGCACCTGGCCCATCAGGCCAGTGGGGCCACAAGGGGCAGAGCCAGGCAAAGTTGTTGGGTCTCCAGAATCCC	2477
AF053327.1	GTCCTTGGCACCTGGCCCATCAGGCCAGTGGGGCCACAAGGGGCAGAGCCAGGCAAAGTTGTTGGGTCTCCAGAATCCC	1389
P2X2-1	GTCCTTGGCACCTGGCCCATCAGGCCAGTGGGGCCACAAGGGGCAGAGCCAGGCAAAGTTGTTGGGTCTCCAGAATCCC	1315
genP2x2f3	GTCCTTGGCACCTGGCCCATCAGGCCAGTGGGGCCACAAGGGGCAGAGCCAGGCAAAGTTGTTGGGTCTCCAGAATCCC	900
 Exon XII		

genP2x2	ACTCCATACCCGCCCTGTCTGAGCAGATAGCGGACACTCCTGACCCGGTGTGTAGGACAAGGGCTTCCCTCTTCTGAGTCG	2557
AF053327.1	ACTCCATACCCG--CCTGTCTGAGCAGATAGCGGACACTCCTGACCCGGTGTGTAGGACAAGGGCTTCCCTCTTCTGAGTCG	1467
P2X2-1	ACTCCATACCCGCCCTGTCTGAGCAGATAGCGGACACTCCTGACCCGGTGTGTAGGACAAGGGCTTCCCTCTTCTGAGTCG	1395
genP2x2f3	ACTCCATACCCGCCCTGTCTGAGCAGATAGCGGACACTCCTGACCCGGTGTGTAGGACAAGGGCTTCCCTCTTCTGAGTCG	980
genP2x2	CCCCTGCAGGACTCCACACCCACAGACCCCAAAGGTTTGGCCAGCTCTGA	2608
AF053327.1	CCCCTGCAGGACTCCACACCCACAGACCCCAAAGGTTTGGCCAGCTCTGAACTTCTGGTCTCACTGTGCTACAGACCT	1547
P2X2-1	CCCCTGCAGGACTCCACACCCACAGACCCCAAAGGTTTGGCCAGCTCTGAACTTCTGGTCTCACTGTGCTACAGACCT	1475
genP2x2f3	CCCCTGCAGGACTCCACACCCACAGACCCCAAAGGTTTGGCCAGCTCTGAACTTCTGGTCTCACTGTGCTACAGACCT	1060

B

		TM1	
P2X2-1	MAATHPKAPTAQRLLAQCWGSFAFDYETPKVIVVNRRL	GVVYRAVQLLILLYFVWVVFIVQKSYQDSETGPSSIITKVK	80
AF053327.1	MAATHPKAPTAQRLLRQG-MSAFWDYETPKVIVVNRRL	GVVYRAVQLLILLYFVWVVFIVQKSYQDSETGPSSIITKVK	79
P2X2-1	GITQSEHKVWDVEEYVKPPEGGSVFSIIITRIEVTTPPQTLGACPEIRVPNTTCHLDADCTAGELDMLGNLRTGRCVPYY		160
AF053327.1	GITQSEHKVWDVEEYVKPPEGGSVFSIIITRIEVTTPPQTLGACPEIRVPNTTCHLDADCTAGELDMLGNLRTGRCVPYY		159
P2X2-1	HGEAKTCEVSGWCPVEDGAAVSHFLGKMAPNFTILIKNSIHYPKFQFSKGNIAHREDDYLRRCTPDQGFDPYCPPIFRLGF		240
AF053327.1	HGEAKTCEVSGWCPVEDGAAVSHFLGKMAPNFTILIKNSIHYPKFQFSKGNIAHRDMTYLRRCTPDQGFDPYCPPIFRLGF		239
P2X2-1	IVEQAGENFTELAHRGGVIGVIINWDCDLLPSSHNCNPKYSFRRLDPKHVPASSGYNFRFAKYRVNSTTTRTLIKAYGI		320
AF053327.1	IVEQAGENFTELAHRGGVIGVIINWDCDLLPSSHNCNPKYSFRRLDPKHVPASSGYNFRFAKYRVNSTTTRTLIKAYGI		319
		TM2	
P2X2-1	RIDVIVHGQAGKFSLIPTIINLATALTSIGVGSFLCDWILLTFMKNKQVYSHKKFDKVCAPSRPSSSWPVTLALILGQAF		400
AF053327.1	RIDVIVHGQAGKFSLIPTIINLATALTSIGVGSFLCDWILLTFMKNKQVYSHKKFDKVCAPSRPSSSWPVTLALILGQAF		399
P2X2-1	PPPRHCSQSLAPGPGQWGPQGAEPGKVVGSPESSHIPALSEQIADTPDRCVGGQLPSSSEPLQDSTPTDPKGLAQI		477
AF053327.1	PPPRHCSQSPWHLAHQAV-GPQGAEPQAKLLGLQNFTPYR-LSEQIADTPDRCVGGQLPSSSEPLQDSTPTDPKGLAQI		474

A) ClustalV alignment of genomic *P2x2* sequence (*genP2x2*) obtained from ENSEMBL (ENSCPOG00000013647) and a segment amplified from guinea pig (*genP2x2f3*) using primers F3 and R1 (see table 3) with P2X2-1 cDNA sequence cloned here and the submitted as AF053327.1. Complete identity along the ORF of P2X2-1 and their corresponding genomic sequence is obtained. Nucleotide sequence differences are marked in blue, start and stop codons are underlined. **B)** ClustalV alignment of the translated protein sequences from P2X2-1 showed above. Identical amino acids are marked in blue. Only the largest P2X2 cDNA (P2X2-1) are showed in the alignment for a better demonstration of the nucleotide differences. Transmembrane domains are indicated as TM1 and TM2.